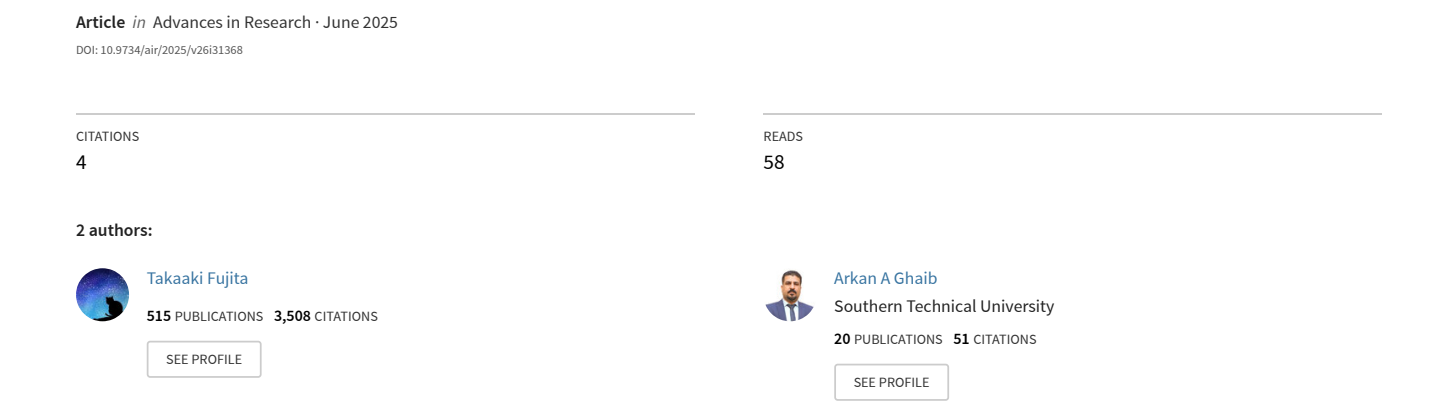
Toward a Unified Theory of Brain Hypergraphs and Symptom Hypernetworks in Medicine and Neuroscience



Advances in Research Advances in Research

Advances in Research

Volume 26, Issue 3, Page 522-565, 2025; Article no.AIR.136474 ISSN: 2348-0394, NLM ID: 101666096

Toward a Unified Theory of Brain Hypergraphs and Symptom Hypernetworks in Medicine and Neuroscience

Takaaki Fujita ${ m a}^*$ and Arkan A. Ghaib ${ m b}$

Independent Researcher, Shinjuku, Shinjuku-ku, Tokyo, Japan.
 Department of Information Technology, Management Technical College, Southern Technical University, Basrah, 61004, Iraq.

Authors' contributions

This work was carried out in collaboration between both authors. Author TF designed the study, analysed and interpreted the findings, and drafted the manuscript. Author AAG reviewed the manuscript and contributed to its writing. Both authors read and approved the final manuscript.

Article Information

DOI: https://doi.org/10.9734/air/2025/v26i31368

Open Peer Review History:

This journal follows the Advanced Open Peer Review policy. Identity of the Reviewers, Editor(s) and additional Reviewers, peer review comments, different versions of the manuscript, comments of the editors, etc are available here: https://pr.sdiarticle5.com/review-history/136474

Received: 01/04/2025 Accepted: 02/06/2025

Published: 11/06/2025

Original Research Article

Cite as: Fujita, Takaaki, and Arkan A. Ghaib. 2025. "Toward a Unified Theory of Brain Hypergraphs and Symptom Hypernetworks in Medicine and Neuroscience". Advances in Research 26 (3):522-65. https://doi.org/10.9734/air/2025/v26i31368.

^{*}Corresponding author: E-mail: takaaki.fujita060@gmail.com;

ABSTRACT

Many biomedical systems exhibit interactions that go beyond simple pairwise connections. A hypergraph generalizes a graph by permitting an edge to connect any number of vertices—such edges are called *hyperedges*. A superhypergraph further extends this concept by recursively nesting powerset layers, enabling multi-level and self-referential relationships.

In neuroscience, Brain Graphs represent pairwise functional or structural connectivity among brain regions, while Symptom Networks capture statistical dependencies among clinical symptoms. In this work, We propose four novel frameworks—*Brain Hypergraphs*, *Symptom Hypernetworks*, *Brain Superhypergraphs*, and *Symptom Superhypernetworks*. For each, We provide rigorous definitions, illustrative examples drawn from real-world biomedical scenarios, and an analysis of their core mathematical properties. These advanced models are specifically designed to represent complex, multi-way, and hierarchical interactions that classical graphs cannot capture.

This paper is devoted to the theoretical formulation and property analysis of these new network structures. We anticipate that future research will implement these frameworks computationally and validate them with domain experts to unlock deeper insights into brain function and disease symptomatology.

Keywords: Graphs, superhypergraphs; hypergraphs; brain hypergraphs; symptom hypernetworks; symptom networks; brain graphs.

1 INTRODUCTION

1.1 Hypergraph and Superhypergraph

Graph theory is a fundamental area of mathematics focused on the study of structures called graphs, in which entities (vertices) are connected by relationships (edges) (Diestel; Deo, 2016; Diestel, 2005). Graph theory is extensively studied across numerous fields. including graph parameters (Robertson and Seymour, 1986; Harvey and Wood, 2017), artificial intelligence (AI), graph algorithms (Velickovic et al., 2019; Swathika et al., 2017; Linial, 1992), graph neural networks (GNNs) (Thiede et al., 2022; Chen and Schwaller, 2024; Li et al., 2024), urban network (Anna Jażdżewska, 2022; Appert and Laurent, 2007; Zhang, 2017), graph signal processing(Fujita, 2025h; Dabush and Routtenberg, 2024; Calazans et al., 2024; Pain et al., 2025), graphic matroids (Bowler et al., 2020; Seymour, 1981), electronics(Fujita, 2025e), material sciences(Fujita, 2025l; Xie and Grossman, 2018; Park and Wolverton, 2020), and chemical graph theory (Fujita and Smarandache; Fujita, 2025g; Cruz et al., 2021; Trinajstic, 2018). Moreover, due to the wide range of applications being explored in graph theory (Gross et al., 2018; Foulds, 1995; Bondy et al., 1976), research in this field is considered highly important.

While traditional graphs connect pairs of vertices, many real-world systems involve more complex, higher-order interactions that cannot be adequately captured

by simple edges. To address this limitation, graph theory has been extended through the concepts of Hypergraphs and superHypergraphs (Fujita, 2025a). A Hypergraph generalizes the classical graph by allowing a single edge-called a hyperedge-to connect any number of vertices simultaneously (Cai et al., 2022; Feng et al., 2019; Bretto, 2013). This makes Hypergraphs especially useful for modeling group-based interactions, such as collaborative teams, biochemical pathways, or co-occurring symptoms. Taking this idea further, a superHypergraph introduces a hierarchy of nested relationships by applying powerset and iterated powerset constructions (Smarandache, 2019, 2020; Fujita, 2025k; Fujita and Smarandache, 2024a). This allows not only for multi-vertex hyperedges but also for higher-level groupings and interactions among hyperedges themselves. These recursive layers are particularly valuable for representing hierarchical, multi-scale, or modular structures.

Such extensions have found applications in both theoretical research and practical domains, including artificial intelligence, social network analysis, and biomedical systems. In network contexts, these generalized structures give rise to *hypernetworks* and *superhypernetworks* (Fujita, 2025c; Hamidi et al., 2023), which serve as network-theoretic analogues of Hypergraphs and superHypergraphs, respectively. They provide a powerful framework for capturing complex, multi-level interactions that go beyond pairwise connectivity.

Table 1. Overview of graph, hypergraph, and superhypergraph

Concept	Notation	Edge Connectivity	Structural Extension
Graph	G = (V, E)	$ \mid E \subseteq \{\{u,v\} \mid u,v \in$	Standard graph: edges
		$V, u \neq v$ (binary edges)	join exactly two vertices.
Hypergraph	H = (V, E)	$E \subseteq \mathcal{P}(V) \setminus \{\emptyset\}$	Generalizes edges to
		(hyperedges)	connect any nonempty
			subset of vertices.
Superhypergraph	$SHT^{(n)} = (V, E)$	$V,E\subseteq \mathcal{P}^n(V_0)$ (super-	Employs n -fold iterated
		vertices and super-	powersets to capture
		edges)	hierarchical, nested
			connectivity among
			edges.

Table 2. Overview of brain graph, brain hypergraph, and brain n-Superhypergraph

Concept	Notation	Vertex Set	Edge/Hyperedge	Key Feature
Brain Graph	G = (V, E)	V: set of ROIs (brain regions)	$ \begin{array}{c c} \textbf{Set} \\ \hline E \subseteq \big\{\{u,v\} \mid \\ u,v \in \\ V, \ \operatorname{corr}(u,v) \geq \\ \tau \big\} \\ \end{array} $	Pairwise functional (or structural) connectivity above a threshold.
Brain Hypergraph	$H = (V, E_H)$	V: set of ROIs	$E_H \subseteq \mathcal{P}(V) \setminus \{\emptyset\}$	Hyperedges encode group-wise co-activation of multiple regions.
Brain n-Superhypergraph	$BSHT^{(n)} = (V^{(n)}, E^{(n)})$	$V^{(n)} \subseteq \mathcal{P}^n(V_0)$: n -supervertices	$E^{(n)}\subseteq \mathcal{P}^n(V_0)$: n -superedges	Recursively nested powerset layers capture multi- level regional modules and their interactions.

Table 1 provides an overview of Graphs, Hypergraphs, and Superhypergraphs. Note that a hyperedge in a hypergraph is a generalized edge that connects any nonempty subset of vertices, representing relationships between nodes. A superedge in an n-SuperHyperGraph is a subset of n-supervertices drawn from the n-th powerset, modeling complex hierarchical multi-level connections. A supervertex in an n-SuperHyperGraph is an element of the n-th iterated powerset of base vertex set, representing nested

groupings. Let n be a natural number. Furthermore, this paper considers only finite concepts.

1.2 Medicine and Graph Theory

Medicine is the science and practice of diagnosing, treating, and preventing illness and disease. Graph theory is also applied in the field of medicine (Sigerist, 1987; Castiglioni, 2019). Due to the significance of this research, graph-based models are also employed

in related disciplines such as biomedicine (Li et al., 2022; Kocbek and Kim, 2017) and medicinal chemistry (Speck-Planche and Cordeiro, 2013; Venhorst et al., 2010; Balasubramanian and Gupta, 2019).

In this paper, We utilize Brain Graphs and Symptom Networks. Brain Graphs represent brain regions as nodes and their functional or structural connections as edges derived from neuroimaging data (Bullmore and Bassett, 2011; Yu et al., 2018; Sporns, 2018; Mhembere et al., 2013). Brain Graphs are widely used in fields such as neuroscience (Bassett and Sporns, 2017; Squire et al., 2012) and continue to be extensively applied in recent studies (Luo et al., 2024; Roobini et al., 2024; Huang et al., 2024). Symptom Networks model symptoms as nodes and statistical associations between them as edges, capturing their interdependencies in medical conditions (van Borkulo et al., 2015; Bergsneider et al., 2024; Senger et al., 2022). Symptom Networks have likewise been the subject of various studies in recent years (Zhu et al., 2023; Bergsneider et al., 2024; Schumacher et al., 2024). Other concepts that can be studied using graphbased approaches include Gene Regulatory Networks (Chen et al., 1999; Karlebach and Shamir, 2008; Madhamshettiwar et al., 2012), Metabolic Pathway Networks (Brown et al., 2016; Milone et al., 2014), Patient Similarity Networks (Pai and Bader, 2018; Pai et al., 2019), Protein-Protein Interaction Networks (Koh et al., 2012; Raman, 2010; Safari-Alighiarloo et al., 2014), and Drug-Target Interaction Networks (Yamanishi et al., 2008; Tanoli et al., 2018; Li et al., 2017). Thus, graph theory also plays a significant role in the field of medicine.

1.3 Proposed Study of This Paper

From the foregoing, Hypernetworks, Hypergraphs, Superhypernetworks, and Superhypergraphs are essential for modeling complex real-world networks, and research on Brain Graphs and Symptom Networks—which have played a major role in practical applications—is likewise important. However, no studies to date have explored Brain Graphs and Symptom Networks through the lens of Hypernetworks, Hypergraphs, Superhypernetworks,

or Superhypergraphs. In this paper, we extend Brain Graphs and Symptom Networks by applying the frameworks of hypergraphs and superhypergraphs. Specifically, we introduce the concepts of Brain Hypergraphs, Symptom Hypernetworks, Brain Superhypergraphs, and Symptom Superhypernetworks, provide concrete examples, and examine their mathematical properties. We anticipate that these extensions will advance research on the medical applications of graph theory. It should be noted that this study is purely theoretical; we hope that future work will incorporate computational experiments and expert validation.

The following presents Table 2: Overview of Brain Graph, Brain Hypergraph, and Brain *n*-Superhypergraph, and Table 3: Overview of Symptom Network, Symptom Hypernetwork, and Symptom SuperHypernetwork. These tables provide an overview of the results presented in this paper.

1.4 Structure of This Paper

This section outlines the structure of the present Section 2 introduces several mathematical definitions, including those of Classical Structure, Hyperstructure, and n-Superhyperstructure, as well as Hypergraph, Superhypergraph, Hypernetwork, and It also defines domainn-SuperHypernetwork. specific constructs such as Brain Graph, Brain Hypergraph, and Symptom Networks. Section 3 presents the definition, illustrative examples, and fundamental properties of the Brain Superhypergraph. Section 4 focuses on the Symptom Hypernetwork and Symptom SuperHypernetwork, discussing their definitions, concrete examples, and key characteristics. Finally, Section 5 provides concluding remarks and a brief discussion of future research directions.

2 PRELIMINARIES AND DEFINITIONS

This section provides an overview of the fundamental concepts and definitions essential for the discussions in this paper. Throughout the paper, We assume all graphs are simple and finite.

Table 3. Overview of symptom network, symptom hypernetwork, and symptom SuperHypernetwork

Concept	Notation	Vertex Set	Edge/Hyperedg	eKey Feature
			Set	
Symptom Network	G = (V, E)	V: set of	$E \subseteq \{\{u,v\} \mid$	Pairwise
		symptoms	$u,v \in$	statistical
			V , assoc $(u, v) \ge$	associations
			$\mid au brace$	(e.g.
				correlations
				or conditional
				probabilities)
Symptom Hypernetwork	$HN = (V, E_H)$	V: set of	$E_H \subseteq \mathcal{P}(V) \setminus$	Hyperedges
		symptoms	{∅}	represent
				frequently
				co-occurring
				symptom
				subsets
				(multivariate
	(7.7(n) -(n)	(m)	-(n) -	dependencies)
Symptom SuperHypernetwork	$SHN^{(n)} = (V^{(n)}, E^{(n)})$	$V^{(n)} \subseteq$	$E^{(n)} \subseteq$	Recursive
		$\mathcal{P}^n(V)$: n-	$\mathcal{P}^n(V)$: n -	grouping of
		supervertices	superedges	symptom
				clusters
				across
				multiple
				scales,
				capturing
				hierarchical
				comorbidity
				patterns

2.1 Classical Structure, Hyperstructure, Definition 2.2 (Subset). (Hausdorff, 2021; Levy, 2012; and *n*-Superhyperstructure

A Classical Structure denotes a general mathematical construct, whereas a Hyperstructure is defined via the powerset(Adebisi and Ajuebishi, 2025; Amiri et al., 2024; Al-Tahan et al., 2021), and an n-Superhyperstructure is defined through the *n*th iterated powerset operation (Das et al., 2025; Al-Odhari, 2025; Smarandache, 2024c,b). Intuitively, the nth powerset arises from repeatedly applying the powerset operator (Smarandache, 2023b, 2024a). Relevant definitions and simple examples are provided below. In this paper, unless stated otherwise, n is assumed to be a natural number. Furthermore, as noted below, the empty set is an element of the powerset of every set.

Definition 2.1 (Set). (Hausdorff, 2021; Levy, 2012; Jech, 2003) A set is a well-defined collection of distinct objects, called elements or members.

Jech, 2003) Let A and B be sets. We say that A is a *subset* of B, written $A \subseteq B$, if every element of A is also an element of B; that is,

$$A \subseteq B \iff \forall x (x \in A \Rightarrow x \in B).$$

Definition 2.3 (Empty Set). Jech (2003) The empty set, denoted by \emptyset , is the unique set that contains no elements. Formally,

$$\emptyset = \{\}$$
 such that $\forall x, x \notin \emptyset$.

Definition 2.4 (Base Set). Fuiita and Smarandache (2025c) A base set S is the foundational set from which complex structures such as powersets and hyperstructures are derived. It is formally defined as:

 $S = \{x \mid x \text{ is an element within a specified domain}\}.$

All elements in constructs like $\mathcal{P}(S)$ or $\mathcal{P}_n(S)$ originate from the elements of S.

Definition 2.5 (Powerset). Fujita and Smarandache (2025c) The *powerset* of a set S, denoted $\mathcal{P}(S)$, is the collection of all possible subsets of S, including both the empty set and S itself. Formally, it is expressed as:

$$\mathcal{P}(S) = \{ A \mid A \subseteq S \}.$$

Example 2.6 (Antihypertensive Therapy Combinations via Powerset). In the management of hypertensionGupta and Guptha (2010); Verma et al. (2021), clinicians may choose among three main classes of antihypertensive agents:

$$S = \{ACEI, TD, BB\},\$$

where

- ACEI = ACE inhibitor (e.g. enalapril),
- TD = thiazide diuretic (e.g. hydrochlorothiazide),
- BB = beta-blocker (e.g. metoprolol).

The powerset $\mathcal{P}(S)$ enumerates all possible therapy regimens:

$$\mathcal{P}(S) = \{ \emptyset, \{ACEI\}, \{TD\}, \{BB\}, \{ACEI, TD\}, \{ACEI, BB\}, \{TD, BB\}, \{ACEI, TD, BB\} \}.$$

- Ø: no pharmacotherapy (lifestyle modification only).
- {ACEI}, {TD}, {BB}: monotherapy with one drug class.
- {ACEI, TD}, {ACEI, BB}, {TD, BB}: dual-drug regimens.
- $\{ACEI, TD, BB\}$: triple-therapy combining all three classes.

This systematic enumeration helps clinicians and clinical trial designers to plan and compare all possible monotherapy, dual-therapy, and triple-therapy strategies, illustrating how the powerset concept applies directly to real-world treatment decision-making.

Definition 2.7 (n-th Powerset). (cf.(Smarandache, 2024b; Fujita and Smarandache, 2025c; Fujita, 2025c; Smarandache, 2022a)) The n-th powerset of a set H, denoted $P_n(H)$, is defined iteratively, starting with the standard powerset. The recursive construction is given by:

$$P_1(H) = P(H), \quad P_{n+1}(H) = P(P_n(H)), \quad \text{for } n \ge 1.$$

Similarly, the n-th non-empty powerset, denoted $P_n^*(H)$, is defined recursively as:

$$P_1^*(H) = P^*(H), \quad P_{n+1}^*(H) = P^*(P_n^*(H)).$$

Here, $P^*(H)$ represents the powerset of H with the empty set removed.

Example 2.8 (Cancer Treatment Protocol Design via n-th Powersets). Cancer treatment protocols are standardized plans outlining therapies (e.g., chemotherapy, radiation, immunotherapy) for specific cancer types and stages (cf.(Gotay et al., 1992; Goodwin et al., 1988)). In oncologyStephens et al. (2009), combination therapy protocols are often organized into multiple treatment cycles. Let the base set of available therapy classes be

$$H = \{\text{Chemo, Targeted, Immuno}\},\$$

where "Chemo" = chemotherapy (cf.DeVita Jr and Chu (2008)), "Targeted" = targeted small-molecule inhibitors, and "Immuno" = immunotherapy (cf.Till et al. (2004)).

First-level therapy combinations $(P_1(H) = \mathcal{P}(H))$: all possible drug combinations within a single cycle:

$$P_1(H) = \{ \emptyset, \{ \text{Chemo} \}, \{ \text{Targeted} \}, \{ \text{Immuno} \}, \}$$

 $\{Chemo, Targeted\}, \{Chemo, Immuno\}, \{Targeted, Immuno\}, \{Chemo, Targeted, Immuno\}\}.$

∅: no drug (supportive care only).

- Single-agent cycles: {Chemo}, {Targeted}, {Immuno}.
- Double-agent cycles, e.g. {Chemo, Targeted}.
- Triple-agent cycle: {Chemo, Targeted, Immuno}.

Second-level regimens $(P_2(H) = \mathcal{P}(P_1(H)))$: sets of cycle-level protocols across multiple cycles. For example, two distinct two-cycle regimens:

$$R_1 = \{\{\text{Chemo}\}, \{\text{Chemo}, \text{Targeted}\}\},\$$
 $R_2 = \{\{\text{Immuno}\}, \{\text{Targeted}, \text{Immuno}\}\}.$

Third-level meta-protocols $(P_3(H) = \mathcal{P}(P_2(H)))$: groupings of multi-cycle regimens, for instance:

$$T = \{R_1, R_2\} \in P_3(H).$$

Thus the hierarchy

$$H \xrightarrow{P_1} \{\text{single-cycle combos}\} \xrightarrow{P_2} \{\text{multi-cycle regimens}\} \xrightarrow{P_3} \{\text{meta-protocols across regimens}\}$$

captures progressively higher "meta" levels of treatment design, from individual cycle combinations to entire multicycle program structures used in clinical trial planning.

Definition 2.9 (Classical Structure). (cf.(Smarandache, 2024b, 2022a)) A *Classical Structure* is a mathematical framework defined on a non-empty set H, equipped with one or more *Classical Operations* that satisfy specified *Classical Axioms*. Specifically:

A Classical Operation is a function of the form:

$$\#_0: H^m \to H,$$

where $m \ge 1$ is a positive integer, and H^m denotes the m-fold Cartesian product of H. Common examples include addition and multiplication in algebraic structures such as groups, rings, and fields.

Definition 2.10 (Hyperoperation). (cf.(Vougioukli, 2020a,b, 2023)) A *hyperoperation* is a generalization of a binary operation where the result of combining two elements is a set, not a single element. Formally, for a set S, a hyperoperation \circ is defined as:

$$\circ: S \times S \to \mathcal{P}(S),$$

where $\mathcal{P}(S)$ is the powerset of S.

Definition 2.11 (Hyperstructure). (cf.(Smarandache, 2024b; Fujita and Smarandache, 2025c; Smarandache, 2022a)) A *Hyperstructure* extends the notion of a Classical Structure by operating on the powerset of a base set. Formally, it is defined as:

$$\mathcal{H} = (\mathcal{P}(S), \circ),$$

where S is the base set, $\mathcal{P}(S)$ is the powerset of S, and \circ is an operation defined on subsets of $\mathcal{P}(S)$. Hyperstructures allow for generalized operations that can apply to collections of elements rather than single elements.

Example 2.12 (Antihypertensive Polypharmacy as a Hyperstructure). Antihypertensive polypharmacy involves using multiple drugs to control high blood pressure effectively and safely (cf.(Bromfield et al., 2017; Falster et al., 2020)). In clinical hypertension management, multiple drug classes are often combined to achieve optimal blood-pressure control. We model recommended drug combinations as a hyperstructure

$$\mathcal{H} = (\mathcal{P}(S), \circ),$$

where the base set of antihypertensive agents is

$$S = \{ACEI, BB, CCB\},\$$

with ACEI = ACE inhibitor, BB = beta-blocker, CCB = calcium-channel blocker.

Hyperoperation o: Define

$$\circ: S \times S \longrightarrow \mathcal{P}(S)$$

on individual agents by evidence-based guidelines:

$$\begin{aligned} & \text{ACEI} \circ \text{BB} = \{\text{ACEI}, \text{BB}\}, \\ & \text{ACEI} \circ \text{CCB} = \{\text{ACEI}, \text{CCB}\}, \\ & \text{BB} \circ \text{CCB} = \{\text{BB}, \text{CCB}\}, \\ & x \circ x = \{x\} \quad (\text{monotherapy}), \\ & x \circ y = \{x, y\} \quad (\text{if no specific guideline exists}). \end{aligned}$$

Extend o to mixtures by

$$A \circ B = \bigcup_{a \in A, b \in B} (a \circ b), \quad A, B \subseteq S.$$

Concrete computations:

$$\{ACEI\} \circ \{BB\} = \{ACEI, BB\},$$

$$\{ACEI, BB\} \circ \{CCB\} = (ACEI \circ CCB) \ \cup \ (BB \circ CCB) = \{ACEI, CCB, BB\}.$$

Thus \mathcal{H} captures clinical polypharmacy: combining any two drug classes yields the recommended dual-therapy set, and mixing dual- and single-agent regimens yields all guideline-endorsed combinations within one algebraic framework.

Definition 2.13 (SuperHyperOperations). (cf.(Smarandache, 2024b)) Let H be a non-empty set, and let $\mathcal{P}(H)$ denote the powerset of H. The n-th powerset $\mathcal{P}^n(H)$ is defined recursively as follows:

$$\mathcal{P}^0(H) = H$$
, $\mathcal{P}^{k+1}(H) = \mathcal{P}(\mathcal{P}^k(H))$, for $k > 0$.

A *SuperHyperOperation* of order (m, n) is an m-ary operation:

$$\circ^{(m,n)}: H^m \to \mathcal{P}^n_*(H),$$

where $\mathcal{P}_*^n(H)$ represents the n-th powerset of H, either excluding or including the empty set, depending on the type of operation:

- If the codomain is $\mathcal{P}^n_*(H)$ excluding the empty set, it is called a *classical-type* (m,n)-SuperHyperOperation.
- If the codomain is $\mathcal{P}^n(H)$ including the empty set, it is called a *Neutrosophic* (m,n)-SuperHyperOperation.

These SuperHyperOperations are higher-order generalizations of hyperoperations, capturing multi-level complexity through the construction of n-th powersets.

Definition 2.14 (n-Superhyperstructure). (cf.(Smarandache, 2024b; Fujita, 2025b; Smarandache, 2022a)) An n-Superhyperstructure further generalizes a Hyperstructure by incorporating the n-th powerset of a base set. It is formally described as:

$$\mathcal{SH}_n = (\mathcal{P}_n(S), \circ),$$

where S is the base set, $\mathcal{P}_n(S)$ is the n-th powerset of S, and \circ represents an operation defined on elements of $\mathcal{P}_n(S)$. This iterative framework allows for increasingly hierarchical and complex representations of relationships within the base set.

Example 2.15 (2-Superhyperstructure of Type 2 Diabetes Management Regimens). Type 2 diabetes is a chronic condition characterized by insulin resistance and high blood glucose levels (cf.(Chatterjee et al., 2017; DeFronzo et al., 2015; Vijan, 2010)). In the management of type 2 diabetes, clinicians combine dietary recommendations, physical activity, and pharmacotherapy in daily and weekly protocols. We model these as a 2-Superhyperstructure

$$SH^{(2)} = (V^{(2)}, \circ),$$

where the base set of interventions is

$$S = \{ \text{Diet, Exercise, Insulin, Metformin} \}.$$

First-level daily regimens $(V^{(1)} \subseteq \mathcal{P}(S))$: choose common daily combinations:

$$\begin{split} D_1 &= \{\text{Diet, Exercise}\}, & D_2 &= \{\text{Diet, Metformin}\}, \\ D_3 &= \{\text{Diet, Insulin}\}, & D_4 &= \{\text{Exercise, Metformin}\}, \\ D_5 &= \{\text{Exercise, Insulin}\}, & D_6 &= \{\text{Diet, Exercise, Metformin}\}. \end{split}$$

Thus

$$V^{(1)} = \{D_1, D_2, D_3, D_4, D_5, D_6\} \subseteq \mathcal{P}(S).$$

Second-level weekly protocols $(V^{(2)} \subseteq \mathcal{P}(\mathcal{P}(S)))$: each W_i is a set of daily regimens used during one week:

$$W_1 = \{D_1, D_2\}, \quad W_2 = \{D_3, D_4\}, \quad W_3 = \{D_5, D_6\}.$$

Hence

$$V^{(2)} = \{W_1, W_2, W_3\} \subseteq \mathcal{P}(V^{(1)}).$$

Superhyperoperation o: Define an operation combining two weekly protocols by

$$W_i \circ W_j = \{ W_i \cup W_j, \ W_i \cap W_j, \ W_i \triangle W_j \}, \quad W_i, W_j \in V^{(2)},$$

where $W_i \triangle W_i$ is the symmetric difference.

Concrete example:

$$W_1 \circ W_2 = \{ \{D_1, D_2, D_3, D_4\}, \{ \}, \{D_1, D_2, D_3, D_4\} \}.$$

Interpretation:

- Each W_i is a 2-supervertex representing a weekly treatment regimen.
- Each element of $W_i \circ W_j$ is a 2-superedge representing possible merged, common, or differential weekly protocols when two regimens are compared.

Thus $(V^{(2)}, \circ)$ models both the design of individual weekly diabetes management plans and their hierarchical interactions, supporting comparison and optimization across multiple protocols.

Example 2.16 (Childhood Immunization Program as a 3-Superhyperstructure). Childhood immunization protects children from infectious diseases through scheduled vaccines, boosting long-term immunity early (cf.(Mathew, 2012; Bangura et al., 2020; Zhou et al., 2014)). Pediatric immunization schedules are planned at three hierarchical levels: vaccine combinations per visit, series of visits over years, and multi-year immunization programs (cf.(Campbell and Burgess, 2004)). We model this as a 3-Superhyperstructure

$$\mathrm{SH}^{(3)} = (\mathcal{P}^3(S), \star),$$

where the base set of vaccine types is

$$S = \{DTP, MMR, Polio\}.$$

First-level visit combinations ($\mathcal{P}^1(S)$):

$$\begin{array}{ll} D_1 = \{ \mathrm{DTP} \}, & D_2 = \{ \mathrm{MMR} \}, & D_3 = \{ \mathrm{Polio} \}, \\ D_4 = \{ \mathrm{DTP}, \mathrm{MMR} \}, & D_5 = \{ \mathrm{DTP}, \mathrm{Polio} \}, & D_6 = \{ \mathrm{MMR}, \mathrm{Polio} \}, \\ D_7 = \{ \mathrm{DTP}, \mathrm{MMR}, \mathrm{Polio} \}. & \end{array}$$

Thus

$$V^{(1)} = \{D_1, D_2, \dots, D_7\} \subseteq \mathcal{P}^1(S).$$

Second-level series regimens $(\mathcal{P}^2(S))$:

$$R_1 = \{D_1, D_4, D_6\}, \quad R_2 = \{D_2, D_5, D_7\}, \quad R_3 = \{D_3, D_4, D_5\}.$$

Hence

$$V^{(2)} = \{R_1, R_2, R_3\} \subseteq \mathcal{P}^2(S).$$

Third-level program modules $(\mathcal{P}^3(S))$:

$$M_1 = \{R_1, R_2\}, \quad M_2 = \{R_2, R_3\}.$$

Thus

$$V^{(3)} = \{M_1, M_2\} \subset \mathcal{P}^3(S).$$

Superhyperoperation *: Combine two program modules by

$$M_i \star M_j = \{ M_i \cup M_j, M_i \cap M_j, M_i \triangle M_j \}, M_i, M_j \in V^{(3)},$$

where $M_i \triangle M_j$ is the symmetric difference.

Concrete example:

$$M_1 \star M_2 = \{ \{R_1, R_2, R_3\}, \{R_2\}, \{R_1, R_3\} \}.$$

Interpretation:

- Each D_k is a possible vaccine combination at one clinic visit.
- Each R_ℓ is a multi-visit regimen across several years.
- Each M_m is a multi-year immunization program combining regimens.
- The operation * yields unified, common, or differential program modules, aiding the comparison and planning of alternative immunization policies.

2.2 Superhypergraph

In classical graph theory, a Hypergraph extends the idea of a conventional graph by permitting edges—called hyperedges—to join more than two vertices. This broader framework enables the modeling of more intricate relationships between elements, thereby enhancing its utility in various fields (Cai et al., 2022; Feng et al., 2019; Berge, 1984; Gottlob and Pichler, 2004). A *Superhypergraph* is an advanced extension of the Hypergraph concept, integrating recursive powerset structures into the classical model. This concept has been recently introduced and extensively studied in the literature (Fujita and Smarandache, 2025a; Fujita, 2024b; Smarandache, 2022b; Valencia et al., 2025; Bravo et al., 2025).

Definition 2.17 (Hypergraph). (Bretto, 2013; Berge, 1984) A *Hypergraph* H = (V(H), E(H)) consists of:

- A nonempty set V(H) of vertices.
- A set E(H) of hyperedges, where each hyperedge is a nonempty subset of V(H), thereby allowing connections among multiple vertices.

Unlike standard graphs, Hypergraphs are well-suited to represent higher-order relationships. In this paper, We restrict ourselves to the case where both V(H) and E(H) are finite.

Example 2.18 (Drug Side-Effect Hypergraph). A drug side-effect is an unintended and typically undesirable effect that occurs in addition to the intended therapeutic outcome (cf. (Pauwels et al., 2011; Ding et al., 2019; Tedla and Bautista, 2016)). We construct a Hypergraph H=(V(H),E(H)) to model the side-effect profiles of three cancer therapies:

 $V(H) = \{$ nausea, alopecia, fatigue, neutropenia, rash, diarrhea, hypertension $\}$,

and

$$E(H) = \{ e_{\text{chemo}}, e_{\text{immuno}}, e_{\text{target}} \},$$

where each hyperedge corresponds to a therapy's observed side effects:

```
e_{
m chemo} = \{ {
m nausea, \ alopecia, \ fatigue, \ neutropenia} \}, \ e_{
m immuno} = \{ {
m fatigue, \ rash, \ diarrhea} \}, \ e_{
m target} = \{ {
m fatigue, \ diarrhea, \ hypertension} \}.
```

Interpretation:

- · Vertices represent individual side effects observed in patients.
- Hyperedges group side effects that co-occur under the same therapy.
- The overlap among hyperedges (e.g. "fatigue" appears in all three therapies) highlights common toxicities, while unique vertices (e.g. "alopecia" for chemotherapy) indicate therapy-specific risks.
- This Hypergraph enables analysis of multi-way side-effect interactions, identification of shared adverse events, and design of combination regimens minimizing overlapping toxicities.

Definition 2.19 (n-Superhypergraph). (Smarandache, 2019, 2020)

Let V_0 be a finite base set of vertices. For each integer $k \geq 0$, define the iterative powerset by

$$\mathcal{P}^{0}(V_{0}) = V_{0}, \quad \mathcal{P}^{k+1}(V_{0}) = \mathcal{P}(\mathcal{P}^{k}(V_{0})),$$

where $\mathcal{P}(\cdot)$ denotes the usual powerset operation. An *n-Superhypergraph* is then a pair

$$SHT^{(n)} = (V, E),$$

with

$$V \subseteq \mathcal{P}^n(V_0)$$
 and $E \subseteq \mathcal{P}^n(V_0)$.

Each element of V is called an *n*-supervertex and each element of E an *n*-superedge.

Example 2.20 (2-Superhypergraph of Therapy Side-Effect Clusters). Therapy side-effect clusters are groups of adverse symptoms that commonly co-occur during medical treatments (cf.(Fried, 2002; Russo and Fried, 2003; Antoni and Braun, 2002)). Let the base set of individual side effects be

 $V_0 = \{$ nausea, alopecia, fatigue, neutropenia, rash, diarrhea, hypertension $\}$.

First-order side-effect profiles (1-supervertices) for three cancer therapies are:

$$e_{\text{chemo}} = \{ \text{nausea}, \text{alopecia}, \text{fatigue}, \text{neutropenia} \},$$

$$e_{\text{immuno}} = \{ \text{fatigue}, \text{rash}, \text{diarrhea} \},$$

 $e_{\text{target}} = \{ \text{fatigue}, \text{diarrhea}, \text{hypertension} \}.$

These lie in $\mathcal{P}^1(V_0)$. We now form two 2-supervertices in $\mathcal{P}^2(V_0)$:

$$U_1 = \{e_{\text{chemo}}, e_{\text{immuno}}\}, \qquad U_2 = \{e_{\text{immuno}}, e_{\text{target}}\}.$$

Thus

$$V = \{ U_1, U_2 \} \subset \mathcal{P}^2(V_0).$$

Under the flattening map flat₂:

$$flat_2(U_1) = e_{chemo} \cup e_{immuno} = \{nausea, alopecia, fatigue, neutropenia, rash, diarrhea\},$$

$$flat_2(U_2) = e_{immuno} \cup e_{target} = \{fatigue, rash, diarrhea, hypertension\}.$$

Next, choose the 2-superedges as subsets of $\mathcal{P}^2(V_0)$:

$$E = \{ \{U_1\}, \{U_2\}, \{U_1, U_2\} \} \subseteq \mathcal{P}^2(V_0).$$

Finally, the 2-Superhypergraph is

$$SHT^{(2)} = (V, E).$$

Interpretation:

- Each 1-supervertex e_* is the set of side effects observed under a single therapy.
- Each 2-supervertex U_j clusters two such therapy profiles, capturing overlapping toxicities.
- A 2-superedge $\{U_1, U_2\}$ links both clusters, representing the union of all side effects across these regimens.
- The flattening map shows how lower-level side-effect sets combine into higher-level clusters, enabling analysis of multi-therapy toxicity patterns.

Example 2.21 (3-Superhypergraph of Cancer Therapy Side-Effect Meta-Clusters). Cancer therapy refers to medical treatments aimed at controlling or eliminating cancer, including surgery, chemotherapy, radiation, immunotherapy, and targeted drug therapies cf. (Semenza, 2003; Cella et al., 1993; Peer et al., 2020b). Let the base set of individual side effects be

 $V_0 = \{$ nausea, alopecia, fatigue, neutropenia, rash, diarrhea, hypertension, arthralgia $\}$.

First-order side-effect profiles (1-supervertices) for four therapies lie in $\mathcal{P}^1(V_0)$:

$$e_{\text{chemo}} = \{\text{nausea, alopecia, fatigue, neutropenia}\}, e_{\text{immuno}} = \{\text{fatigue, rash, diarrhea, arthralgia}\},$$

$$e_{\text{target}} = \{ \text{fatigue}, \text{diarrhea}, \text{hypertension} \}, e_{\text{endo}} = \{ \text{fatigue}, \text{arthralgia}, \text{hypertension} \}.$$

Next, form two 2-supervertices in $\mathcal{P}^2(V_0)$:

$$U_1 = \{e_{\text{chemo}}, e_{\text{immuno}}\}, \quad U_2 = \{e_{\text{target}}, e_{\text{endo}}\}.$$

Under the flattening map flat₂:

$$\operatorname{flat}_2(U_1) = e_{\operatorname{chemo}} \cup e_{\operatorname{immuno}} = \{ \operatorname{nausea}, \operatorname{alopecia}, \operatorname{fatigue}, \operatorname{neutropenia}, \operatorname{rash}, \operatorname{diarrhea}, \operatorname{arthralgia} \},$$

$$\operatorname{flat}_2(U_2) = e_{\operatorname{target}} \cup e_{\operatorname{endo}} = \{ \operatorname{fatigue}, \operatorname{diarrhea}, \operatorname{hypertension}, \operatorname{arthralgia} \}.$$

Finally, choose two 3-supervertices in $\mathcal{P}^3(V_0)$:

$$W_1 = \{ U_1 \}, \qquad W_2 = \{ U_2 \}.$$

Thus

$$V = \{ W_1, W_2 \} \subseteq \mathcal{P}^3(V_0), \quad E = \{ \{ W_1 \}, \{ W_2 \}, \{ W_1, W_2 \} \} \subseteq \mathcal{P}^3(V_0).$$

Interpretation:

- Each 1-supervertex \boldsymbol{e}_* is the set of side effects under one therapy.
- Each 2-supervertex U_j clusters two therapy profiles, capturing overlapping toxicities across those regimens.
- Each 3-supervertex W_k wraps a 2-supervertex into the next hierarchical layer, enabling grouping of side-effect clusters themselves.
- The 3-superedges $\{W_1\}$ and $\{W_2\}$ represent individual meta-clusters, while $\{W_1, W_2\}$ models the union of both meta-clusters across all therapies.
- The flattening map flat_3 recovers the full set of side effects: $\text{flat}_3(W_1) = \text{flat}_2(U_1)$, etc., illustrating how raw side effects propagate through three levels of hierarchical grouping.

2.3 Hypernetwork and *n*-SuperHypernetwork

A hypernetwork extends graphs by allowing hyperedges to connect multiple nodes, modeling complex multi-way relationships between entities. An n-SuperHypernetwork uses nested powersets of nodes to represent hierarchical multi-level interactions and groupings in complex systems.

Definition 2.22 (Network). A network (or graph) is an ordered triple

$$N = (V, E, w)$$

where

- *V* is a nonempty finite set of *vertices* (or *nodes*);
- $E \subseteq \{\{u,v\} \mid u,v \in V, u \neq v\}$ is the set of *undirected edges*, each joining two distinct vertices;
- $w: E \to \mathbb{R}_{\geq 0}$ is a *weight function* assigning a nonnegative real weight to each edge (omitted if unweighted).

If edges are directed, one instead writes

$$N = (V, A, w), \quad A \subseteq V \times V,$$

and each $(u,v) \in A$ is an *arc* from u to v. In either case, one may also include an optional *vertex-labeling* $\ell_V : V \to L_V$ to record vertex types.

Definition 2.23 (Hypernetwork). (cf.(Aksoy et al., 2020; Ha et al., 2016; Chauhan et al., 2024; Fujita, 2025c)) A *hypernetwork* is an ordered triple

$$H = (V, \mathcal{E}, w)$$

where

- *V* is a nonempty finite set of *nodes*;
- E ⊆ P(V)\{∅} is the set of hyperedges, each hyperedge e ∈ E being a nonempty subset of nodes (allowing multi-node interactions);
- $w \colon \mathcal{E} \to \mathbb{R}_{\geq 0}$ is a *weight or attribute function* on hyperedges (omitted if unweighted).

A directed hypernetwork may be defined by replacing $\mathcal{E} \subseteq \mathcal{P}(V)$ with a set of ordered tuples of nodes or by equipping each $e \in \mathcal{E}$ with a head-tail partition. One can further add a node-labeling $\ell_V: V \to L_V$ and a hyperedge-labeling $\ell_{\mathcal{E}}: \mathcal{E} \to L_{\mathcal{E}}$ to record types or properties.

Example 2.24 (Drug Combination Hypernetwork in Oncology). Drug combination refers to the use of two or more medications together to enhance therapeutic effectiveness or reduce side effects (cf.Chou (2010, 2006)). Consider a set of four chemotherapeutic agents commonly used in breast cancer treatment:

 $V = \{ \text{Doxorubicin (Doxo) (cf.Carvalho et al. (2009))}, \text{ Paclitaxel (Pacli) (cf.Singla et al. (2002))},$

Cisplatin (Cis) (cf.Loehrer and EINHORN (1984)), 5-Fluorouracil (5-FU) (cf.Longley et al. (2003)) }.

We define hyperedges corresponding to experimentally tested drug combinations, with weights given by the Combination Index (CI), where CI < 1 indicates synergy:

$$\mathcal{E} = \big\{ \{\, \mathsf{Doxo}, \mathsf{Pacli}\}, \,\, \{\, \mathsf{Doxo}, \mathsf{Cis}, \mathsf{5}\text{-}\mathsf{FU}\},$$

{ Pacli, 5-FU} }.

Let $w: \mathcal{E} \to \mathbb{R}_{\geq 0}$ assign:

$$w(\{\mathsf{Doxo}, \mathsf{Pacli}\}) = \mathrm{CI}_{\mathsf{Doxo}+\mathsf{Pacli}} = 0.78,$$

$$w(\{\mathsf{Doxo}, \mathsf{Cis}, \mathsf{5}\text{-}\mathsf{FU}\}) = \mathrm{CI}_{\mathsf{Doxo}+\mathsf{Cis}+\mathsf{5}\text{-}\mathsf{FU}} = 0.65,$$

$$w(\{\text{Pacli}, 5\text{-FU}\}) = \text{CI}_{\text{Pacli}+5\text{-FU}} = 0.85.$$

Then the Drug Combination Hypernetwork is

$$H_{\rm drug} = (V, \mathcal{E}, w).$$

- Node set ${\cal V}$ represents individual chemotherapeutic agents.
- Hyperedges in \mathcal{E} represent multi-drug regimens tested in vitro.
- Weight w(e) is the measured Combination Index for the regimen e, quantifying synergistic efficacy.
- For example, $w(\{Doxo, Cis, 5-FU\}) = 0.65$ indicates strong three-drug synergy.

This hypernetwork model captures higher-order interactions among drugs, facilitating identification of synergistic combinations that may improve treatment outcomes.

Definition 2.25 (n-SuperHypernetwork). (Fujita, 2025c) Let V_0 be a finite base set of *nodes*. Define the n-th iterated powerset recursively by

$$\mathcal{P}^{0}(V_{0}) = V_{0}, \qquad \mathcal{P}^{k+1}(V_{0}) = \mathcal{P}(\mathcal{P}^{k}(V_{0})) \quad (k \ge 0).$$

An *n-superhypernetwork* is a tuple

$$\mathcal{N}^{(n)} = (V, \mathcal{E}, w)$$

where

- $V \subseteq \mathcal{P}^n(V_0)$ is a finite set of *n*-supernodes;
- $\mathcal{E} \subseteq \mathcal{P}^n(V_0)$ is a finite set of *n*-superedges, each superedge $e \in \mathcal{E}$ being a nonempty subset of V;
- $w: \mathcal{E} \to \mathbb{R}_{\geq 0}$ is an optional *weight function* assigning a nonnegative real weight (or confidence) to each superedge.

In other words, both vertices and hyperedges of the network are drawn from the n-th powerset of the base node set, capturing up to n levels of hierarchical grouping.

Example 2.26 (2-SuperHypernetwork of Multi-Modal Cancer Therapies). (cf.(Xu et al., 2022)) Cancer therapy involves medical treatments such as surgery, chemotherapy, radiation, immunotherapy, or targeted drugs to eliminate or control cancer (cf.(Peer et al., 2020a; Kerr et al., 1994; Brown and Giaccia, 1998; Brigger et al., 2012)). Consider four principal treatment modalities for a solid tumor:

$$V_0 = \{ \text{Chemo, Radio, Immuno, Target} \},$$

where "Chemo" = chemotherapy (cf.(DeVita Jr and Chu, 2008)), "Radio" = radiotherapy (cf.Nair et al. (2001)), "Immuno" = immunotherapy (cf.(Till et al., 2004)), and "Target" = targeted small-molecule therapy (cf.(Wang et al., 2024)). We record clinical synergy indices for first-order combinations (1-supernodes):

$$\mathcal{P}^1(V_0) = \mathcal{P}(V_0), \quad v_a = \{\text{Chemo, Radio}\}, \ v_b = \{\text{Immuno, Target}\}, \ v_c = \{\text{Chemo, Immuno, Target}\}.$$

Numeric synergy (higher = better) estimates from phase II trials:

$$\sigma(v_a) = 1.4, \quad \sigma(v_b) = 1.7, \quad \sigma(v_c) = 2.0.$$

Form two 2-supernodes in $\mathcal{P}^2(V_0)$:

$$V^{(2)} = \mathcal{P}^2(V_0) \supseteq \{ U_1, U_2 \},\$$

where

$$U_1 = \{ v_a, v_b \}, \quad U_2 = \{ v_b, v_c \}.$$

Under the flattening map flat2:

$$\text{flat}_2(U_1) = v_a \cup v_b = \{\text{Chemo}, \text{Radio}, \text{Immuno}, \text{Target}\}, \quad \text{flat}_2(U_2) = v_b \cup v_c = \{\text{Chemo}, \text{Immuno}, \text{Target}\}.$$

We then define the Symptom 2-SuperHypernetwork (here, Therapy 2-SuperHypernetwork)

$$\mathcal{N}^{(2)} = (V^{(2)}, \mathcal{E}^{(2)}, w^{(2)}),$$

with

$$\mathcal{E}^{(2)} = \{\{U_1\}, \{U_2\}, \{U_1, U_2\}\},\$$

and weight function

$$w^{(2)}(\{U_1\}) = \frac{\sigma(v_a) + \sigma(v_b)}{2} = \frac{1.4 + 1.7}{2} = 1.55,$$

$$w^{(2)}(\{U_2\}) = \frac{\sigma(v_b) + \sigma(v_c)}{2} = \frac{1.7 + 2.0}{2} = 1.85,$$

$$w^{(2)}(\{U_1, U_2\}) = \frac{\sigma(v_a) + 2\sigma(v_b) + \sigma(v_c)}{4} = \frac{1.4 + 2 \cdot 1.7 + 2.0}{4} = 1.70.$$

Here:

- Each 1-supernode v_i is a specific drug combination.
- Each 2-supernode U_i clusters two such combinations representing treatment regimens tested in parallel.
- Weights $\boldsymbol{w}^{(2)}$ represent average synergy across the clustered regimens.
- The 2-superedge $\{U_1, U_2\}$ models the joint interaction of both regimen clusters.

This 2-SuperHypernetwork captures not only individual drug synergies but also how different combination strategies group and interact at a higher hierarchical level, aiding selection of optimal multi-modal therapy protocols.

Example 2.27 (Stroke Rehabilitation Program as a 3-SuperHypernetwork). In post-stroke care(Rajsic et al., 2019; Hempler et al., 2018; Whitehead and Baalbergen, 2019), rehabilitation combines multiple therapies (physical, occupational, speech, and cognitive) in daily sessions, weekly modules, and monthly phases. We model this as a 3-SuperHypernetwork

$$\mathcal{N}^{(3)} = (V^{(3)}, \mathcal{E}^{(3)}, w^{(3)}),$$

where the base set of therapy modalities is

$$V_0 = \{\text{PT, OT, ST, CT}\},\$$

with PT = physical therapy, OT = occupational therapy, ST = speech therapy, CT = cognitive therapy.

First-level session combinations $(V^{(1)} \subseteq \mathcal{P}(V_0))$:

$$S_1 = \{PT, OT\}, \quad S_2 = \{PT, ST\}, \quad S_3 = \{OT, CT\},$$

$$V^{(1)} = \{S_1, S_2, S_3\}.$$

Second-level weekly modules $(V^{(2)} \subseteq \mathcal{P}(\mathcal{P}(V_0)))$:

$$W_1 = \{S_1, S_2\}, \quad W_2 = \{S_2, S_3\}, \quad V^{(2)} = \{W_1, W_2\}.$$

Third-level monthly phases $(V^{(3)} \subseteq \mathcal{P}^3(V_0))$:

$$M_1 = \{W_1\}, \quad M_2 = \{W_2\}, \quad M_3 = \{W_1, W_2\}, \quad V^{(3)} = \{M_1, M_2, M_3\}.$$

Superhyperedges ($\mathcal{E}^{(3)} \subseteq \mathcal{P}^3(V_0)$):

$$\mathcal{E}^{(3)} = \{\{M_1, M_3\}, \{M_2, M_3\}\}.$$

Weight function $w^{(3)}: \mathcal{E}^{(3)} \to [0,1]$ (e.g. patient-reported adherence):

$$w^{(3)}(\{M_1, M_3\}) = 0.82, \quad w^{(3)}(\{M_2, M_3\}) = 0.75.$$

Interpretation:

- Level 1 ($V^{(1)}$): daily therapy sessions combining two modalities.
- Level 2 ($V^{(2)}$): weekly modules grouping session types.
- Level 3 ($V^{(3)}$): monthly rehabilitation phases composed of weekly modules.
- Each superhyperedge $\{M_i, M_3\}$ links a single-module phase with the comprehensive combined phase, with $w^{(3)}$ quantifying average patient adherence or functional gain.

Thus $\mathcal{N}^{(3)}$ captures the hierarchical organization of rehabilitation protocols from individual sessions up to integrated monthly programs, facilitating analysis of adherence and efficacy across multiple scales.

2.4 Brain Graph and Brain Hypergraph

A brain graph represents brain regions as nodes and functional connections—typically based on BOLD signal similarity—as weighted or unweighted edges. The definition of the Brain Graph is presented as follows.

Definition 2.28 (Brain Graph). Let

$$V = \{v_1, v_2, \dots, v_N\}$$

be a set of brain regions (Regions of Interest, ROIs), and let

 $\mathbf{x}_i = [x_i(t_1), \dots, x_i(t_T)]^{\top} \in \mathbb{R}^T$ be the BOLD time-series for region v_i . Define a similarity function $\kappa : \mathbb{R}^T \times \mathbb{R}^T \to \mathbb{R}$ (e.g. Pearson correlation). For a threshold $\tau \in [0,1]$, the functional connectivity matrix $\mathbf{A} \in \mathbb{R}^{N \times N}$ has entries

$$A_{ij} = \begin{cases} \kappa(\mathbf{x}_i, \mathbf{x}_j), & \kappa(\mathbf{x}_i, \mathbf{x}_j) \geq \tau, \\ 0, & \text{otherwise.} \end{cases}$$

The brain graph is the undirected graph

$$G = (V, E), \quad E = \{\{v_i, v_j\} : A_{ij} > 0\}.$$

Example 2.29 (Resting-State fMRI Brain Graph). Resting-state fMRI measures brain activity by detecting spontaneous blood flow fluctuations during rest(cf.(Smith et al., 2013; Smitha et al., 2017; Lee et al., 2013)). A common real-world example constructs a brain graph from resting-state fMRI data in the Human Connectome Project:

- Nodes $V=\{v_1,\ldots,v_{90}\}$ are 90 cortical and subcortical regions defined by the Automated Anatomical Labeling (AAL) atlas.
- Time-series $\mathbf{x}_i \in \mathbb{R}^T$ for each region v_i is the average BOLD signal over T=300 time points.
- Similarity $\kappa(\mathbf{x}_i, \mathbf{x}_j)$ is the Pearson correlation r_{ij} .

• Choose threshold $\tau = 0.3$. The adjacency matrix has

$$A_{ij} = \begin{cases} r_{ij}, & r_{ij} \ge 0.3, \\ 0, & \text{otherwise.} \end{cases}$$

• The resulting brain graph G=(V,E) has edges $E=\{\{v_i,v_j\}:A_{ij}>0\}$, e.g. strong connections appear among the Posterior Cingulate (v_{PCC}) , Medial Prefrontal Cortex (v_{mPFC}) , and Angular Gyrus (v_{AG}) , forming the Default Mode Network subgraph.

This graph reveals community structure, small-worldness, and hub regions characterizing healthy functional organization.

Brain Hypergraph represents multiple brain regions as nodes and their groupwise co-activation patterns as hyperedges based on neuroimaging data (cf. (Cai et al., 2023; Wu et al., 2022; Pisarchik et al., 2024)). The definition of the Brain Hypergraph is presented as follows.

Definition 2.30 (Brain Hypergraph). (cf. (Cai et al., 2023; Wu et al., 2022; Pisarchik et al., 2024)) Let V and $\{\mathbf{x}_i\}$ be as above. Choose a threshold τ and a multivariate co-activation measure $\zeta: \underbrace{\mathbb{R}^T \times \cdots \times \mathbb{R}^T}_{k \text{ times}} \to \mathbb{R}$. Define the

set of hyperedges

$$\mathcal{E} = \{e = \{v_{i_1}, \dots, v_{i_k}\} \subseteq V : \zeta(\mathbf{x}_{i_1}, \dots, \mathbf{x}_{i_k}) \ge \tau\}.$$

Then the brain Hypergraph is the pair

$$H = (V, \mathcal{E}).$$

with incidence matrix $H \in \left\{0,1\right\}^{N \times |\mathcal{E}|}$ given by

$$H_{i\ell} = \begin{cases} 1, & v_i \in e_\ell, \\ 0, & \text{otherwise.} \end{cases}$$

Example 2.31 (Working-Memory Task Brain Hypergraph). Working memory is the brain's system for temporarily holding and manipulating information necessary for reasoning, learning, and decision-making (cf. (Linden, 2007; McAllister et al., 1999)). In a working-memory experiment, one can build a brain Hypergraph capturing high-order co-activations:

- Nodes V = {DLPFC, PCC, SPL, Hipp, Thal} are five key ROIs (Dorsolateral Prefrontal Cortex, Posterior Cingulate, Superior Parietal Lobule, Hippocampus, Thalamus).
- For each trial, extract BOLD responses $\mathbf{x}_i \in \mathbb{R}^T$ during the 2 s memory-maintenance period.
- Define a multivariate co-activation measure $\zeta(\mathbf{x}_i,\mathbf{x}_j,\mathbf{x}_k)$ as the three-way partial correlation.
- With threshold $\tau = 0.2$, collect all triples $\{v_i, v_j, v_k\}$ whose $\zeta \geq 0.2$. For instance:

$$e_1 = \{ DLPFC, Hipp, Thal \}, e_2 = \{ PCC, SPL, Hipp \}.$$

• The brain Hypergraph is $H=(V,\mathcal{E})$ with $\mathcal{E}=\{e_1,e_2,\dots\}$. Here e_1 links the prefrontal-hippocampal-thalamic memory circuit, while e_2 captures parietal-hippocampal coupling during spatial maintenance.

This Hypergraph model highlights groupings of three or more regions working together, beyond pairwise connectivity, to support working-memory function.

Proposition 2.32 (Validity of Brain Hypergraph). Let $H = (V, \mathcal{E})$ be defined as above. Then H is a hypergraph in the sense that

$$\mathcal{E} \subseteq \mathcal{P}(V) \setminus \{\emptyset\},\$$

and each hyperedge $e \in \mathcal{E}$ satisfies $|e| \geq 2$ and $\zeta(\mathbf{x}_{i_1}, \dots, \mathbf{x}_{i_k}) \geq \tau > 0$.

Proof. By definition,

$$\mathcal{E} = \{ e \subseteq V : \zeta(\mathbf{x}_{i_1}, \dots, \mathbf{x}_{i_k}) \ge \tau \}.$$

Each such e is nonempty and, since ζ is only evaluated on groups of size $k \geq 2$, actually satisfies $|e| \geq 2$. Hence $\mathcal{E} \subseteq \mathcal{P}(V) \setminus \{\emptyset\}$, fulfilling the definition of a hypergraph.

Proposition 2.33 (2-Section Recovers Brain Graph). *Define the* 2-section *(or* clique expansion) $G_2 = (V, E_2)$ of the brain hypergraph $H = (V, \mathcal{E})$ by

$$E_2 = \{\{v_i, v_j\} \subseteq V : \exists e \in \mathcal{E} \text{ with } \{v_i, v_j\} \subseteq e\}.$$

Then G_2 coincides with the thresholded brain graph G = (V, E) constructed at the same threshold τ .

Proof. If $\{v_i, v_j\} \in E$ in the brain graph, then $\kappa(\mathbf{x}_i, \mathbf{x}_j) \geq \tau$. Choosing k = 2 and $\zeta = \kappa$, we get $\{v_i, v_j\} \in \mathcal{E}$. Conversely, if $\{v_i, v_j\} \subseteq e \in \mathcal{E}$ with |e| = k, then by monotonicity of typical co-activation measures one has $\kappa(\mathbf{x}_i, \mathbf{x}_j) \geq \tau$. Thus exactly the same pairs appear in E_2 and in E.

Proposition 2.34 (Induced Subhypergraph). Let $U \subseteq V$ be any nonempty subset of brain regions. Define

$$\mathcal{E}_U = \{ e \in \mathcal{E} : e \subseteq U \}.$$

Then (U, \mathcal{E}_U) is itself a valid brain hypergraph on the sub-set of regions U.

Proof. Since $U \subseteq V$, every $e \in \mathcal{E}_U$ is a nonempty subset of U with $|e| \geq 2$ and $\zeta(\mathbf{x}_{i_1}, \ldots) \geq \tau$. Hence $\mathcal{E}_U \subseteq \mathcal{P}(U) \setminus \{\emptyset\}$, and the same co-activation criterion applies. Thus (U, \mathcal{E}_U) satisfies all hypergraph axioms.

Proposition 2.35 (Connectivity Inheritance). If the brain graph G = (V, E) is connected, then the 2-section G_2 of the hypergraph $H = (V, \mathcal{E})$ is also connected.

Proof. Connectivity of G means every pair v_i, v_j is joined by a path of edges each satisfying $\kappa(\mathbf{x}_p, \mathbf{x}_q) \geq \tau$. By Proposition 2.33, each such edge arises from some hyperedge in \mathcal{E} . Hence in G_2 those same pairs are adjacent. Concatenating these adjacencies reproduces the path in G, showing G_2 is connected.

2.5 Symptom Network

A Symptom Network models symptoms as nodes and their statistical or causal associations as edges, revealing interdependencies in medical conditions. The definition of the Symptom network is presented as follows.

Definition 2.36 (Symptom Network). Let $S = \{s_1, \ldots, s_N\}$ be a set of N symptoms, and let $\mathbf{X} = (X_1, \ldots, X_N)$ be a multivariate random vector where X_i encodes the presence or severity of symptom s_i . A *symptom network* is an undirected, weighted graph

$$G = (V, E, W)$$

with

$$V = S$$
, $E \subseteq \{\{s_i, s_j\} : i \neq j\}$, $W = (w_{ij})_{i,j=1}^N$,

where each weight

$$w_{ij} = \begin{cases} \operatorname{association}(X_i, X_j \mid \mathbf{X}_{\backslash \{i, j\}}), & \{s_i, s_j\} \in E, \\ 0, & \text{otherwise}, \end{cases}$$

quantifies the direct conditional association between X_i and X_j given all other symptoms (e.g. a nonzero Gaussian partial correlation, or a nonzero regularized logistic-regression coefficient).

Example 2.37 (Depressive Symptom Network from EURO-D Data). (cf.(An et al., 2019)) Following Van Borkulo *et al.*, one may estimate a symptom network for late-life depression using the EURO-D scale (12 binary items) on N=8,557 older adults. Denote symptoms s_1-s_{12} (e.g. depressed mood, pessimism, sleep problems, etc.). Using the eLASSO method (logistic regressions with L₁-penalty and EBIC model selection), each symptom s_i is regressed on all others to obtain a sparse set of neighbors. The resulting undirected network G=(V,E,W) has

$$V = \{s_1, \dots, s_{12}\}, \quad w_{ij} = \hat{\beta}_{ij},$$

where $\hat{\beta}_{ij}$ is the estimated penalty-regularized coefficient linking s_i and s_j . In this network:

- Nodes s_1 (death wishes), s_2 (depressed mood), s_3 (loss of interest), and s_4 (pessimism) have the highest *strength* centrality.
- Edges are drawn only if $\hat{\beta}_{ij} \neq 0$, with thickness proportional to $|\hat{\beta}_{ij}|$.
- Central symptoms form feedback loops sustaining the syndrome and suggest targets for focused interventions.

Proposition 2.38 (Symmetry and Simplicity). Let G = (S, E, W) be a Symptom Network as defined above. Then:

- 1. $w_{ij} = w_{ji}$ for all i, j.
- 2. $w_{ii} = 0$ for all i, and there are no self-loops.

Proof. By construction, w_{ij} is a conditional association measure between X_i and X_j . Such measures (e.g. Gaussian partial correlation or logistic-regression coefficient) are symmetric in i and j, so $w_{ij} = w_{ji}$. Moreover, we only define edges for $i \neq j$, and set $w_{ii} = 0$. Hence G is a simple, undirected, weighted graph with no self-loops and symmetric weights.

Proposition 2.39 (Induced Subnetwork). Let $U \subseteq S$ be any nonempty subset of symptoms. Define

$$E_U = \{ \{s_i, s_j\} \in E : s_i, s_j \in U \}, \quad W_U = (w_{ij})_{s_i, s_j \in U}.$$

Then (U, E_U, W_U) is itself a valid Symptom Network on the symptom set U.

Proof. Since $U \subseteq \mathcal{S}$, each pair $\{s_i, s_j\} \subseteq U$ that was an edge in G remains an undirected edge in the induced subnetwork. The weight w_{ij} is unchanged. Definitionally, conditional association can be restricted to the subvector \mathbf{X}_U , and the same threshold criterion applies. Thus (U, E_U, W_U) satisfies all requirements of a Symptom Network.

Proposition 2.40 (Thresholding Yields Subnetwork). For any $\theta > 0$, define

$$E(\theta) = \{ \{s_i, s_j\} \in E : |w_{ij}| \ge \theta \}, \quad W(\theta) = (w_{ij})_{\{s_i, s_j\} \in E(\theta)}.$$

Then $(S, E(\theta), W(\theta))$ is a Symptom Network that is a subgraph of G.

Proof. Since $\theta > 0$, the set $E(\theta) \subseteq E$ consists of those edges whose absolute association exceeds θ . The graph remains simple and undirected, and weights are nonnegative (or real) as before. All defining properties are preserved, so the thresholded graph is a smaller Symptom Network on \mathcal{S} .

Proposition 2.41 (Gaussian Graphical Model Correspondence). Suppose $\mathbf{X} \sim N(0, \Sigma)$ is multivariate normal with precision matrix $\Theta = \Sigma^{-1}$. If we take

$$w_{ij} = - \, \frac{\Theta_{ij}}{\sqrt{\Theta_{ii} \, \Theta_{jj}}} \quad \text{and} \quad E = \big\{ \{s_i, s_j\} : \Theta_{ij} \neq 0 \big\},$$

then G = (S, E, W) is exactly the conditional-independence graph of X.

Proof. A well-known result in Gaussian graphical models states that $X_i \perp X_j \mid \mathbf{X}_{\backslash \{i,j\}}$ if and only if $\Theta_{ij} = 0$. Moreover, the partial correlation between X_i and X_j is given by $-\Theta_{ij}/\sqrt{\Theta_{ii}\,\Theta_{jj}}$. Hence defining w_{ij} in this way yields the exact conditional association, and the edge-set E matches the nonzero entries of Θ . Therefore G recovers the Gaussian conditional-independence graph.

3 RESULTS: BRAIN n-SUPERHYPERGRAPH

The definition of the Brain n-Superhypergraph is presented as follows.

Definition 3.1 (Brain n-Superhypergraph). Let $V_0 = \{r_1, \dots, r_N\}$ be a set of brain regions (ROIs). For each $k \ge 0$ define

$$\mathcal{P}^{0}(V_{0}) = V_{0}, \qquad \mathcal{P}^{k+1}(V_{0}) = \mathcal{P}(\mathcal{P}^{k}(V_{0})).$$

A Brain n-Superhypergraph is a pair

$$BSHT^{(n)} = (V^{(n)}, E^{(n)}),$$

where

$$V^{(n)} \subseteq \mathcal{P}^n(V_0)$$
 (the *n*-supervertices), $E^{(n)} \subseteq \mathcal{P}^n(V_0)$ (the *n*-superedges),

together with the incidence set

$$I = \{(v, e) : v \in V^{(n)}, e \in E^{(n)}, v \in e\},\$$

and attachment maps $\pi(v, e) = v$, e(v, e) = e.

Example 3.2 (Brain 2-Superhypergraph of Resting-State Co-Activation Networks). Resting-State Co-Activation Networks represent spontaneous brain region interactions during rest, revealing intrinsic functional connectivity patterns via neuroimaging data (cf.An et al. (2024); Kaiser et al. (2019)). Let the base set of regions be

$$V_0 = \{PCC, mPFC, AG, ACC, Ins, Hipp\},\$$

where PCC = Posterior Cingulate Cortex, mPFC = medial Prefrontal Cortex, AG = Angular Gyrus, ACC = Anterior Cingulate Cortex, Ins = Insula, and Hipp = Hippocampus.

Level-1 Hypergraph (Brain Hypergraph). Define three co-activation hyperedges based on resting-state networks:

$$\begin{split} e_1 &= \{ \text{PCC, mPFC, AG} \} \quad \text{(Default Mode Network)}, \\ e_2 &= \{ \text{mPFC, ACC, Ins} \} \quad \text{(Salience Network)}, \\ e_3 &= \{ \text{ACC, Ins, Hipp} \} \quad \text{(Memory Network)}. \end{split}$$

Thus the Brain Hypergraph is $H^{(1)} = (V_0, \{e_1, e_2, e_3\}).$

Level-2 supervertices. We form 2-supervertices by grouping pairs of hyperedges that overlap:

$$D_1 = \{e_1, e_2\}$$
 since $e_1 \cap e_2 = \{mPFC\},\$

$$D_2 = \{e_2, e_3\}$$
 since $e_2 \cap e_3 = \{ACC, Ins\}.$

No other hyperedges overlap, so

$$V^{(2)} = \{D_1, D_2\}.$$

Level-2 superedges. There is a single 2-superedge connecting D_1 and D_2 , because they both contain e_2 :

$$E^{(2)} = \{\{D_1, D_2\}\}.$$

Hence the Brain 2-Superhypergraph is

$$BSHT^{(2)} = (V^{(2)}, E^{(2)}) = (\{\{e_1, e_2\}, \{e_2, e_3\}\}, \{\{\{e_1, e_2\}, \{e_2, e_3\}\}\}\}).$$

This 2-superHypergraph encodes a higher-order "meta-network" linking the Default Mode, Salience, and Memory networks via their shared co-activated regions.

Example 3.3 (Brain 2-Superhypergraph of a Sensorimotor–Attention Meta-Network). Sensorimotor refers to the integrated processes involving sensory input and motor output, enabling perception, coordination, and interaction with the environment (cf. (Wolpert et al., 1995; Henderson, 2001)). Let the base set of regions be

$$V_0 = \{M1, SMA, PMC, S1, PPC, V5, FEF\},\$$

where:

- M1 = Primary Motor Cortex
- SMA = Supplementary Motor Area
- PMC = Premotor Cortex
- S1 = Primary Somatosensory Cortex
- PPC = Posterior Parietal Cortex
- V5 = Area MT (Motion-Selective Visual)
- FEF = Frontal Eye Field

Level-1 hyperedges (co-activation networks). Define four co-activation hyperedges based on known functional circuits:

 $e_1 = \{ \mathrm{M1, SMA, PMC} \}$ (Motor Execution Network), $e_2 = \{ \mathrm{S1, M1, PPC} \}$ (Sensorimotor Integration), $e_3 = \{ \mathrm{V5, M1, PPC} \}$ (Visual–Motor Coordination), $e_4 = \{ \mathrm{PPC, SMA, FEF} \}$ (Spatial Attention Network).

Thus the Brain Hypergraph is

$$H^{(1)} = (V_0, \{e_1, e_2, e_3, e_4\}).$$

Level-2 supervertices. Group overlapping hyperedges into 2-supervertices:

$$\begin{split} &D_1 = \{\,e_1, e_2\}, & \text{(overlap on M1)}, \\ &D_2 = \{\,e_2, e_3\}, & \text{(overlap on M1, PPC)}, \\ &D_3 = \{\,e_3, e_4\}, & \text{(overlap on PPC)}, \\ &D_4 = \{\,e_4, e_1\}, & \text{(overlap on SMA)}. \end{split}$$

Hence

$$V^{(2)} = \{D_1, D_2, D_3, D_4\}.$$

Level-2 superedges. Connect those 2-supervertices that share a common level-1 hyperedge:

$$E^{(2)} = \{\{D_1, D_2\}, \{D_2, D_3\}, \{D_3, D_4\}, \{D_4, D_1\}\}.$$

Therefore, the Brain 2-Superhypergraph is

$$BSHT^{(2)} = (V^{(2)}, E^{(2)}),$$

which forms a 4-cycle in the meta-network space, encoding how the Motor Execution, Sensorimotor Integration, Visual–Motor Coordination, and Spatial Attention circuits interlink via shared regions.

Theorem 3.4 (Reduction to Brain Hypergraph and Brain Graph). Let $\mathrm{BSHT}^{(n)} = (V^{(n)}, E^{(n)})$ be a Brain n-Superhypergraph. Then:

1. For n=1, $V^{(1)}\subseteq \mathcal{P}(V_0)$ and $E^{(1)}\subseteq \mathcal{P}(V_0)$, so $\mathrm{BSHT}^{(1)}$ coincides with the standard Brain Hypergraph (V_0,\mathcal{E}) , where each $e\in E^{(1)}$ is a co-activation hyperedge.

2. For n=0, $V^{(0)} \subseteq V_0$ and $E^{(0)} \subseteq V_0$, hence $\mathrm{BSHT}^{(0)}$ reduces to the Brain Graph $G=(V_0,E)$, with edges defined by pairwise functional connectivity above threshold.

Proof. (1) When n=1, by definition $V^{(1)} \subseteq \mathcal{P}(V_0)$ and $E^{(1)} \subseteq \mathcal{P}(V_0)$. Identifying each 1-supervertex with the single region it contains recovers the Brain Hypergraph structure of co-activated region sets.

(2) When n=0, $\mathcal{P}^0(V_0)=V_0$. Thus $V^{(0)}\subseteq V_0$ and $E^{(0)}\subseteq V_0$. Interpreting each 0-superedge $\{r_i,r_j\}$ as an undirected edge gives the Brain Graph defined by thresholded pairwise correlations.

Theorem 3.5 (Intrinsic n-Superhypergraph Structure). Every Brain n-Superhypergraph $\operatorname{BSHT}^{(n)} = (V^{(n)}, E^{(n)})$ is by construction an n-Superhypergraph: its supervertex set $V^{(n)}$ and superedge set $E^{(n)}$ satisfy

$$V^{(n)} \subseteq \mathcal{P}^n(V_0), \quad E^{(n)} \subseteq \mathcal{P}^n(V_0),$$

with the natural incidence relation.

Proof. By definition, $V^{(n)}$ and $E^{(n)}$ are subsets of $\mathcal{P}^n(V_0)$. The incidence set I pairs each supervertex v with exactly those superedges e that contain it. This data precisely matches the requirements of an n-Superhypergraph, with no further structure needed.

Theorem 3.6 (Skeleton Consistency). Let $\mathrm{BSHT}^{(n)} = (V^{(n)}, E^{(n)})$ be a Brain n-Superhypergraph over base node set V_0 . Define for each $k = n - 1, n - 2, \ldots, 0$:

$$V^{(k)} \ = \ \bigcup_{S \in V^{(k+1)}} S, \qquad E^{(k)} \ = \ \big\{ \, F \subseteq V^{(k)} : F \subseteq e \text{ for some } e \in E^{(k+1)} \big\}.$$

Then for every k, $(V^{(k)}, E^{(k)})$ is itself a Brain k-Superhypergraph. In particular:

- $(V^{(1)}, E^{(1)})$ recovers the standard Brain Hypergraph.
- $(V^{(0)}, E^{(0)})$ is the Brain Graph.

Proof. We proceed by downward induction. For k=n, the statement is true by hypothesis. Assume $(V^{(k+1)}, E^{(k+1)})$ is a Brain (k+1)-Superhypergraph with $V^{(k+1)} \subseteq \mathcal{P}^{k+1}(V_0)$, $E^{(k+1)} \subseteq \mathcal{P}^{k+1}(V_0)$. Then

$$V^{(k)} = \bigcup_{S \in V^{(k+1)}} S \subseteq \bigcup_{S \in \mathcal{P}^{k+1}(V_0)} S = \mathcal{P}^k(V_0),$$

and each $F \in E^{(k)}$ satisfies $F \subseteq e$ for some $e \in E^{(k+1)}$, hence $F \subseteq \mathcal{P}^k(V_0)$. The natural membership incidence makes $(V^{(k)}, E^{(k)})$ a valid Brain k-Superhypergraph. Iterating down to k = 0 establishes the result.

Theorem 3.7 (Connectivity Inheritance). If the Brain Graph (the 0-skeleton $(V^{(0)}, E^{(0)})$) is connected, then for every $1 \le k \le n$, the 2-section graph of the Brain k-Superhypergraph $(V^{(k)}, E^{(k)})$ is also connected.

Proof. The 2–section of a Hypergraph has an edge between two supervertices whenever they share at least one lower–level vertex. For k=0, the 2–section is the Brain Graph, which is connected by assumption. Assume the 2–section at level k-1 is connected. At level k, any two k-supervertices S,T that overlap in a (k-1)-supervertex become adjacent in the 2–section. Since the (k-1)–level 2–section is connected, there is a path of overlapping supervertices linking S and T. Thus the level-k 2–section is connected. By induction, connectivity is inherited up to level n.

Theorem 3.8 (Subedge-Induced Functional Connectivity). In a Brain n-Superhypergraph $\mathrm{BSHT}^{(n)} = (V^{(n)}, E^{(n)})$, each n-superedge $e \in E^{(n)}$ induces a connected subgraph in the underlying Brain Graph on the union of its base-level regions.

Proof. Let $e \in E^{(n)}$ be an n-superedge. By skeleton consistency (Theorem 3.6), e corresponds to a collection of (n-1)-supervertices whose union forms a connected subgraph in the 2–section at level n-1. Recursively applying the same argument down to level 0 shows that the union of the base regions in e is connected in the Brain Graph, since overlapping at each level guarantees adjacency at the next lower level. Hence the induced subgraph is connected.

Theorem 3.9 (Converse of Reduction to Brain Hypergraph and Brain Graph).

1. Let $H = (V_0, \mathcal{E})$ be any Brain Hypergraph. Then setting

$$V^{(1)} = \mathcal{E}, \quad E^{(1)} = \mathcal{E} \subset \mathcal{P}^1(V_0)$$

vields a Brain 1-Superhypergraph $BSHT^{(1)} = (V^{(1)}, E^{(1)})$ whose reduction (skeleton at k = 1) recovers H.

2. Let $G = (V_0, E)$ be any Brain Graph. Then setting

$$V^{(0)} = V_0, \quad E^{(0)} = E \subseteq \mathcal{P}^0(V_0)$$

yields a Brain 0-Superhypergraph $BSHT^{(0)} = (V^{(0)}, E^{(0)})$ whose reduction at k = 0 recovers G.

Proof. (1) By hypothesis $H=(V_0,\mathcal{E})$. Take $V^{(1)}=\mathcal{E}\subseteq\mathcal{P}(V_0)$ and $E^{(1)}=\mathcal{E}$ as in the statement. Then BSHT⁽¹⁾ is a valid 1-Superhypergraph by Definition 2.11, and its skeleton at level 1 is exactly (V_0,\mathcal{E}) . (2) For a Brain Graph $G=(V_0,E)$, note $\mathcal{P}^0(V_0)=V_0$. Thus choosing $V^{(0)}=V_0$ and $E^{(0)}=E\subseteq V_0$ gives a valid

0-Superhypergraph. Its reduction at k=0 is precisely the original graph G.

Theorem 3.10 (Converse Connectivity Inheritance). Let $\mathrm{BSHT}^{(n)} = (V^{(n)}, E^{(n)})$ be a Brain n-Superhypergraph over V_0 . If for some $1 \le k \le n$ the 2-section graph of level k,

$$2\sec(V^{(k)}, E^{(k)}),$$

is connected, then the 0-skeleton Brain Graph $(V^{(0)}, E^{(0)})$ is also connected.

Proof. By Theorem 3.6 (Skeleton Consistency), each lower-level skeleton is obtained by "flattening" from level k down to level 0. If the 2-section at level k is connected, then every pair of k-supervertices is joined by a chain of overlapping supervertices. Each overlap in turn ensures adjacency in the (k-1)-level 2-section, and so on by downward induction until level 0. Hence the brain graph $(V^{(0)}, E^{(0)})$ inherits connectivity.

4 RESULTS: SYMPTOM HYPERNETWORK AND SYMPTOM SUPER-HYPERNETWORK

We propose novel mathematical definitions for the *Symptom Hypernetwork* and the *Symptom n-SuperHypernetwork*, and examine their structural properties. Formal definitions, theoretical results, and several illustrative examples are presented in the following subsections.

4.1 Symptom Hypernetwork

The definition and properties of the Symptom Hypernetwork are described below.

Definition 4.1 (Symptom Hypernetwork). Let

$$S = \{s_1, \ldots, s_N\}$$

be a finite set of symptoms, and let $\mathbf{X} = (X_1, \dots, X_N)$ be the corresponding multivariate random vector. Define

$$\mathcal{E} = \{ e \subseteq \mathcal{S} : |e| \ge 2, \operatorname{assoc}(X_e \mid \mathbf{X}_{\mathcal{S} \setminus e}) \ne 0 \},$$

where $\operatorname{assoc}(X_e \mid \mathbf{X}_{S \setminus e})$ is any suitable measure of conditional joint-association among the variables $\{X_i : i \in e\}$ given all other symptoms. Then the *Symptom Hypernetwork* is the hypernetwork

$$H_{\text{sym}} = (\mathcal{S}, \mathcal{E}, w),$$

with weight function $w \colon \mathcal{E} \to \mathbb{R}_{\geq 0}$ defined by

$$w(e) = |\operatorname{assoc}(X_e \mid \mathbf{X}_{S \setminus e})|.$$

Example 4.2 (Symptom Hypernetwork for Migraine Headache). Migraine headache is a recurrent neurological condition causing intense, throbbing head pain, often with nausea, sensitivity to light, and aura (cf.Gilmore and Michael (2011a); Binfalah et al. (2018); Karimi et al. (2017)). Consider a study of N=200 migraine patients, where We record the presence (1) or absence (0) of four key symptoms:

$$S = \{ s_1 = \text{Headache}, s_2 = \text{Nausea}, s_3 = \text{Photophobia}, s_4 = \text{Dizziness} \}.$$

Let $\mathbf{X} = (X_1, X_2, X_3, X_4)$ denote the corresponding binary random vector. We estimate:

· Pairwise conditional associations by Gaussian partial correlation:

$$\rho_{ij} = \operatorname{corr}(X_i, X_j \mid X_{S \setminus \{s_i, s_i\}}).$$

· Triple-wise conditional association by conditional mutual information:

$$I_{ijk} = I(X_i, X_j, X_k \mid X_{S \setminus \{s_i, s_j, s_k\}}).$$

We then form the hyperedge set

$$\mathcal{E} = \{ e \subseteq \mathcal{S} : |e| \ge 2, \operatorname{assoc}(X_e \mid X_{\mathcal{S} \setminus e}) \ne 0 \},$$

with weights

$$w(e) = \begin{cases} |\rho_{ij}|, & e = \{s_i, s_j\}, \\ I_{ijk}, & e = \{s_i, s_j, s_k\}. \end{cases}$$

A concrete estimate yields:

$$\rho_{12} = 0.45, \ \rho_{13} = 0.60, \ \rho_{24} = 0.30, \quad I_{134} = 0.12,$$

and all other associations fall below our significance threshold. Hence

$$\mathcal{E} = \{\{s_1, s_2\}, \{s_1, s_3\}, \{s_2, s_4\}, \{s_1, s_3, s_4\}\}.$$

The resulting Symptom Hypernetwork is

$$H_{\text{migraine}} = (\mathcal{S}, \mathcal{E}, w),$$

where, for example,

$$w({s_1, s_3}) = 0.60, \quad w({s_1, s_3, s_4}) = 0.12.$$

This model captures not only pairwise conditional dependencies among symptoms but also a significant three-way interaction between headache, photophobia, and dizziness, which classical networks would miss.

Example 4.3 (Symptom Hypernetwork for Acute Ischemic Stroke). Acute ischemic stroke presents with a range of neurological deficits whose co-occurrence patterns can guide diagnosis and treatment planning. In a cohort of N=300 stroke patients, We record presence (1) or absence (0) of five key symptoms:

 $\mathcal{S} = \{ \mathit{s}_1 = \mathsf{Facial\ Droop}, \ \mathit{s}_2 = \mathsf{Arm\ Weakness}, \ \mathit{s}_3 = \mathsf{Speech\ Difficulty}, \ \mathit{s}_4 = \mathsf{Vision\ Loss}, \ \mathit{s}_5 = \mathsf{Headache} \}.$

Let $\mathbf{X} = (X_1, \dots, X_5)$ be the corresponding binary random vector. We estimate:

· Pairwise conditional association by partial correlation:

$$\rho_{ij} = \operatorname{corr}(X_i, X_j \mid \mathbf{X}_{\mathcal{S} \setminus \{s_i, s_i\}}).$$

• Triple-wise association by conditional mutual information:

$$I_{ijk} = I(X_i, X_j, X_k \mid \mathbf{X}_{S \setminus \{s_i, s_i, s_k\}}).$$

A concrete estimation yields:

$$\rho_{12} = 0.62, \quad \rho_{13} = 0.48, \quad \rho_{25} = 0.35, \quad I_{123} = 0.18, \quad I_{145} = 0.11,$$

with all other associations below significance. Hence the hyperedge set is

$$\mathcal{E} = \{\{s_1, s_2\}, \{s_1, s_3\}, \{s_2, s_5\}, \{s_1, s_2, s_3\}, \{s_1, s_4, s_5\}\},\$$

and the weights are

$$w(e) = \begin{cases} |\rho_{ij}|, & e = \{s_i, s_j\}, \\ I_{ijk}, & e = \{s_i, s_j, s_k\}. \end{cases}$$

Thus the Stroke Symptom Hypernetwork is

$$H_{\text{stroke}} = (\mathcal{S}, \mathcal{E}, w),$$

where, for example, $w(\{\text{Facial Droop}, \text{Arm Weakness}\}) = 0.62$ and $w(\{\text{Facial Droop}, \text{Vision Loss}, \text{Headache}\}) = 0.11$.

This hypernetwork captures both pairwise conditional dependencies—such as between facial droop and arm weakness—and significant three-way interactions (e.g. facial droop, vision loss, and headache), which would be missed by ordinary networks.

Theorem 4.4. The Symptom Hypernetwork H_{sym} is a Hypernetwork.

Proof. By construction:

- The node-set $\mathcal S$ is a nonempty finite set.
- The hyperedge-set \mathcal{E} satisfies $\mathcal{E} \subseteq \mathcal{P}(\mathcal{S}) \setminus \{\emptyset\}$ and each $e \in \mathcal{E}$ is nonempty.
- The function $w: \mathcal{E} \to \mathbb{R}_{\geq 0}$ assigns a nonnegative real to each hyperedge.

These are precisely the requirements of a hypernetwork (V, \mathcal{E}, w) (cf. Definition of Hypernetwork), so H_{sym} is indeed a hypernetwork.

Theorem 4.5 (Generalization of the Symptom Network). If We restrict the Symptom Hypernetwork $H_{\text{sym}} = (\mathcal{S}, \mathcal{E}, w)$ to only pairwise hyperedges,

$$\mathcal{E}_2 = \{ \{s_i, s_j\} \in \mathcal{E} : |\{s_i, s_j\}| = 2 \}, \quad w_2 = w|_{\mathcal{E}_2},$$

then (S, \mathcal{E}_2, w_2) coincides with the classical Symptom Network.

Proof. By definition of \mathcal{E} , $\{s_i,s_j\}\in\mathcal{E}_2$ exactly when $\mathrm{assoc}(X_i,X_j\mid \mathbf{X}_{\mathcal{S}\setminus\{i,j\}})\neq 0$. Thus \mathcal{E}_2 and w_2 match the edge-set and weight-matrix of the original Symptom Network $G=(\mathcal{S},E,W)$. Hence the Symptom Hypernetwork strictly generalizes the Symptom Network.

Theorem 4.6 (Induced Subhypernetwork). Let $H_{\mathrm{sym}} = (\mathcal{S}, \mathcal{E}, w)$ be a Symptom Hypernetwork, and let $T \subseteq \mathcal{S}$ be any nonempty subset of symptoms. Define

$$\mathcal{E}_T = \{ e \in \mathcal{E} : e \subseteq T \}, \quad w_T = w \big|_{\mathcal{E}_T}.$$

Then

$$H_T = (T, \mathcal{E}_T, w_T)$$

is itself a valid Symptom Hypernetwork.

Proof. By construction:

- T is a nonempty finite set.
- $\mathcal{E}_T \subseteq \mathcal{P}(T) \setminus \{\emptyset\}$ and each $e \in \mathcal{E}_T$ satisfies $|e| \geq 2$ and $\operatorname{assoc}(X_e \mid \mathbf{X}_{S \setminus e}) \neq 0$.
- $w_T : \mathcal{E}_T \to \mathbb{R}_{\geq 0}$ assigns to each e the same nonnegative weight w(e).

These conditions match the definition of a Symptom Hypernetwork, hence H_T is indeed a hypernetwork on T. \Box

Theorem 4.7 (Clique Expansion (2-Section) Representation). Let $H_{\text{sym}} = (\mathcal{S}, \mathcal{E}, w)$ be a Symptom Hypernetwork. Define its 2-section graph $G_2 = (\mathcal{S}, E_2, w_2)$ by

$$E_2 = \{\{s_i, s_i\} \subseteq \mathcal{S} : \exists e \in \mathcal{E} \text{ with } \{s_i, s_i\} \subseteq e\},\$$

$$w_2(\{s_i, s_j\}) = \max_{\substack{e \in \mathcal{E} \\ \{s_i, s_j\} \subseteq e}} w(e).$$

Then G_2 is a well-defined weighted Symptom Network that captures all pairwise associations implied by the hyperedges.

Proof. First, $E_2 \subseteq \{\{s_i, s_j\} : s_i \neq s_j\}$ is finite and nonempty whenever H_{sym} contains at least one hyperedge of size ≥ 2 . Second, for each $\{s_i, s_j\} \in E_2$, there exists at least one $e \in \mathcal{E}$ with $\{s_i, s_j\} \subseteq e$, so the maximum in the definition of w_2 is taken over a nonempty finite set of nonnegative numbers and hence is well-defined and nonnegative. Thus (\mathcal{S}, E_2, w_2) satisfies the definition of a weighted Symptom Network, proving the claim.

Theorem 4.8 (Connectivity Inheritance). If the incidence bipartite graph of the Symptom Hypernetwork

$$B = (\mathcal{S} \cup \mathcal{E}, \{(s, e) : s \in e\})$$

is connected, then its 2-section graph G_2 (as in Theorem 4.7) is also connected.

Proof. In the incidence graph B, symptoms and hyperedges alternate along any path. Connectivity of B implies that for any two symptoms s_i, s_j , there is a path

$$s_i - e_{i_1} - s_{i_2} - e_{i_2} - \cdots - e_{i_k} - s_j.$$

Projecting this path onto symptoms alone yields a sequence where each consecutive pair $\{s_{i_\ell}, s_{i_{\ell+1}}\}$ lies together in some hyperedge e_{i_ℓ} . By Theorem 4.7, each such pair is an edge in G_2 . Concatenating these edges produces a path from s_i to s_j in G_2 , establishing connectivity.

4.2 Symptom SuperHypernetwork

The definition and properties of the Symptom SuperHypernetwork are described below.

Definition 4.9 (Symptom n-SuperHypernetwork). Let $S = \{s_1, \ldots, s_N\}$ be a finite set of symptoms, and let $\mathbf{X} = (X_1, \ldots, X_N)$ be the corresponding multivariate random vector. Define recursively

$$\mathcal{P}^0(\mathcal{S}) = \mathcal{S}, \quad \mathcal{P}^{k+1}(\mathcal{S}) = \mathcal{P}(\mathcal{P}^k(\mathcal{S})) \quad (k \ge 0).$$

Also define the flattening map

$$\operatorname{flat}_1(e) = e \subseteq \mathcal{S}, \quad \operatorname{flat}_{k+1}(E) = \bigcup_{e \in E} \operatorname{flat}_k(e) \quad (E \subseteq \mathcal{P}^{k+1}(\mathcal{S})).$$

Then set

$$V^{(n)} = \mathcal{P}^n(\mathcal{S}), \quad \mathcal{E}^{(n)} = \Big\{ e \subseteq V^{(n)} : \big| \text{flat}_n(e) \big| \ge 2, \ \operatorname{assoc} \big(X_{\text{flat}_n(e)} \mid \mathbf{X}_{\mathcal{S} \setminus \text{flat}_n(e)} \big) \ne 0 \Big\},$$

and define the weight function

$$w^{(n)} : \mathcal{E}^{(n)} \to \mathbb{R}_{\geq 0}, \quad w^{(n)}(e) = |\operatorname{assoc}(X_{\operatorname{flat}_n(e)} \mid \mathbf{X}_{\mathcal{S} \setminus \operatorname{flat}_n(e)})|.$$

The Symptom n-SuperHypernetwork is then

$$H_{\text{sym}}^{(n)} = (V^{(n)}, \mathcal{E}^{(n)}, w^{(n)}).$$

Example 4.10 (Symptom 2-SuperHypernetwork for Migraine Headache). Migraine headache is a neurological disorder causing intense throbbing pain, often accompanied by nausea, light sensitivity, and visual disturbances (cf.Gilmore and Michael (2011b); Stewart et al. (1992); Hansen et al. (2012)). Let

$$S = \{ s_1 = \text{Headache}, s_2 = \text{Nausea}, s_3 = \text{Photophobia}, s_4 = \text{Dizziness} \}$$

and $\mathbf{X} = (X_1, X_2, X_3, X_4)$ the corresponding binary random vector recorded on N = 200 patients. From the Symptom Hypernetwork (Example 4.2), We have estimated:

$$\rho_{12} = 0.45, \ \rho_{13} = 0.60, \ \rho_{24} = 0.30, \quad I_{123} = 0.12, \ I_{134} = 0.10, \quad I_{1234} = 0.08.$$

Define the iterated powersets

$$\mathcal{P}^0(\mathcal{S}) = \mathcal{S}, \quad \mathcal{P}^1(\mathcal{S}) = \mathcal{P}(\mathcal{S}), \quad \mathcal{P}^2(\mathcal{S}) = \mathcal{P}(\mathcal{P}(\mathcal{S})).$$

Select two 2-supernodes from $\mathcal{P}^2(\mathcal{S})$:

$$v_1 = \{\{s_1, s_2\}, \{s_1, s_3\}\}, \quad v_2 = \{\{s_2, s_4\}, \{s_1, s_3, s_4\}\}.$$

Under the flattening map flat2:

$$flat_2(v_1) = \{s_1, s_2, s_3\}, \quad flat_2(v_2) = \{s_1, s_2, s_3, s_4\}.$$

We then form the Symptom 2-SuperHypernetwork

$$H_{\text{migraine}}^{(2)} = (V^{(2)}, \mathcal{E}^{(2)}, w^{(2)}),$$

where

$$V^{(2)} = \mathcal{P}^2(\mathcal{S}), \qquad \mathcal{E}^{(2)} = \{\{v_1\}, \{v_2\}, \{v_1, v_2\}\},\$$

and the weight function $w^{(2)}$ is given by

$$w^{(2)}(\{v_1\}) = \left|\operatorname{assoc}(X_{\{1,2,3\}} \mid X_{\{4\}})\right| = I_{123} = 0.12,$$

$$w^{(2)}(\{v_2\}) = \left|\operatorname{assoc}(X_{\{1,2,3,4\}} \mid X_{\emptyset})\right| = I_{1234} = 0.08,$$

$$w^{(2)}(\{v_1, v_2\}) = \left|\operatorname{assoc}(X_{\{1,2,3,4\}} \mid X_{\emptyset})\right| = I_{1234} = 0.08.$$

Here:

- Each 2-supernode v_i is a cluster of symptom-clusters (1-supernodes).
- Hyperedges $\{v_1\}$ and $\{v_2\}$ capture significant three-way and four-way associations.
- Hyperedge $\{v_1, v_2\}$ models the joint interaction between the two higher-order symptom clusters.

This 2-SuperHypernetwork thus encodes not only pairwise and triple interactions but also how these interactions group at a second hierarchical level, revealing multi-scale dependency structure among migraine symptoms.

Example 4.11 (Symptom 2-SuperHypernetwork for Influenza-Like Illness). Influenza-like illness is a clinical condition marked by fever, cough, sore throat, and fatigue, resembling symptoms of seasonal influenza (cf.Kelly and Birch (2004); Babcock et al. (2006); Bulgakova et al. (2018)). Consider N=5 common symptoms of influenza-like illness:

$$S = \{ s_1 = \text{Fever}, \ s_2 = \text{Cough}, \ s_3 = \text{SoreThroat}, \ s_4 = \text{Fatigue}, \ s_5 = \text{Headache} \},$$

and let $\mathbf{X} = (X_1, \dots, X_5)$ be the corresponding binary random vector for N = 300 patients. From empirical estimation We obtain:

$$\rho_{12}=0.55,\;\rho_{14}=0.50,\;\rho_{23}=0.40,\;\rho_{35}=0.45,\quad I_{124}=0.18,\;I_{345}=0.12,\;I_{12345}=0.05.$$

Define the iterated powersets

$$\mathcal{P}^0(\mathcal{S}) = \mathcal{S}, \quad \mathcal{P}^1(\mathcal{S}) = \mathcal{P}(\mathcal{S}), \quad \mathcal{P}^2(\mathcal{S}) = \mathcal{P}\big(\mathcal{P}(\mathcal{S})\big).$$

Select two 2-supernodes in $\mathcal{P}^2(\mathcal{S})$:

$$v_1 = \{\{s_1, s_2\}, \{s_1, s_4\}\}, \quad v_2 = \{\{s_3, s_5\}, \{s_2, s_3, s_4\}\}.$$

Under the flattening map $flat_2$:

$$flat_2(v_1) = \{s_1, s_2, s_4\}, \quad flat_2(v_2) = \{s_2, s_3, s_4, s_5\}.$$

We then form the Symptom 2-SuperHypernetwork

$$H_{\text{flu}}^{(2)} = (V^{(2)}, \mathcal{E}^{(2)}, w^{(2)}),$$

where

$$V^{(2)} = \mathcal{P}^2(\mathcal{S}), \qquad \mathcal{E}^{(2)} = \{\{v_1\}, \{v_2\}, \{v_1, v_2\}\},\$$

and the weight function is

$$w^{(2)}(\{v_1\}) = \left|\operatorname{assoc}(X_{\{1,2,4\}} \mid X_{\{3,5\}})\right| = I_{124} = 0.18,$$

$$w^{(2)}(\{v_2\}) = \left|\operatorname{assoc}(X_{\{2,3,4,5\}} \mid X_{\{1\}})\right| = I_{345} = 0.12,$$

$$w^{(2)}(\{v_1, v_2\}) = \left|\operatorname{assoc}(X_{\{1,2,3,4,5\}} \mid X_{\emptyset})\right| = I_{12345} = 0.05.$$

Here:

- Each 2-supernode v_i clusters lower-level symptom interactions into a higher-order group.
- Hyperedges $\{v_1\}$ and $\{v_2\}$ capture the significant triple and quadruple associations respectively.
- The hyperedge $\{v_1, v_2\}$ reflects the full five-way interaction among all symptoms.

This 2-SuperHypernetwork reveals multi-scale dependency structures in influenza-like illness, beyond pairwise and triple associations.

Example 4.12 (Symptom 3-SuperHypernetwork for COVID-19 Symptoms). COVID-19 symptoms include fever, cough, fatigue, loss of taste or smell, and difficulty breathing, varying in severity among individuals (cf.Johansson et al. (2021); Nguyen et al. (2020); Peghin et al. (2021)). Let

$$S = \{ s_1 = \text{Fever}, \ s_2 = \text{Cough}, \ s_3 = \text{Fatigue}, \ s_4 = \text{Anosmia}, \ s_5 = \text{Headache} \}$$

and $\mathbf{X}=(X_1,X_2,X_3,X_4,X_5)$ the corresponding binary indicator vector recorded on N=500 patients. From empirical estimation We obtain:

$$\rho_{34} = \operatorname{corr}(X_3, X_4 \mid X_{\{1,2,5\}}) = 0.35, \quad I_{125} = I(X_1, X_2, X_5 \mid X_{\{3,4\}}) = 0.07, \quad I_{12345} = I(X_1, \dots, X_5 \mid \emptyset) = 0.03.$$

We construct:

$$\mathcal{P}^0(\mathcal{S}) = \mathcal{S}, \quad \mathcal{P}^1(\mathcal{S}) = \mathcal{P}(\mathcal{S}), \quad \mathcal{P}^2(\mathcal{S}) = \mathcal{P}(\mathcal{P}(\mathcal{S})), \quad \mathcal{P}^3(\mathcal{S}) = \mathcal{P}(\mathcal{P}^2(\mathcal{S})).$$

Define two 2-supernodes in $\mathcal{P}^2(\mathcal{S})$:

$$u_1 = \{\{s_1, s_2\}, \{s_2, s_5\}\}, \quad u_2 = \{\{s_3, s_4\}\}.$$

Then two 3-supernodes in $\mathcal{P}^3(\mathcal{S})$:

$$v_1 = \{ u_1 \}, \quad v_2 = \{ u_2 \}.$$

Under the flattening map $flat_k$:

$$flat_3(v_1) = flat_2(u_1) = \{s_1, s_2\} \cup \{s_2, s_5\} = \{s_1, s_2, s_5\}, \quad flat_3(v_2) = flat_2(u_2) = \{s_3, s_4\}.$$

We then form the Symptom 3-SuperHypernetwork

$$H_{\text{covid}}^{(3)} = (V^{(3)}, \mathcal{E}^{(3)}, w^{(3)}),$$

where

$$V^{(3)} = \mathcal{P}^3(\mathcal{S}), \quad \mathcal{E}^{(3)} = \{\{v_1\}, \{v_2\}, \{v_1, v_2\}\}.$$

The weight function $w^{(3)}$ is defined by

$$w^{(3)}(\{v_1\}) = \left|\operatorname{assoc}(X_{\{1,2,5\}} \mid X_{\{3,4\}})\right| = I_{125} = 0.07,$$

$$w^{(3)}(\{v_2\}) = \left|\operatorname{assoc}(X_{\{3,4\}} \mid X_{\{1,2,5\}})\right| = |\rho_{34}| = 0.35,$$

$$w^{(3)}(\{v_1, v_2\}) = \left|\operatorname{assoc}(X_{\{1, \dots, 5\}} \mid \emptyset)\right| = I_{12345} = 0.03.$$

Here:

- The 2-supernode u_1 groups the two boundary interactions $\{s_1, s_2\}$ and $\{s_2, s_5\}$, and v_1 wraps u_1 into a 3-supernode capturing the triple association among fever, cough, and headache.
- The 2-supernode u_2 contains the pair $\{s_3, s_4\}$, and v_2 wraps it to capture the fatigue—anosmia interaction.
- The 3-superedge $\{v_1,v_2\}$ models the full five-symptom interaction, revealing the global dependency structure among all COVID-19 symptoms.

This 3-SuperHypernetwork thus encodes hierarchical symptom interactions across three levels, from pairwise boundaries up to full syndrome interdependence.

Theorem 4.13. The structure $H_{\text{sym}}^{(n)}$ defined above is an n-SuperHypernetwork.

Proof. By construction:

- 1. $V^{(n)} \subseteq \mathcal{P}^n(\mathcal{S})$ is finite and nonempty.
- 2. $\mathcal{E}^{(n)} \subseteq \mathcal{P}(V^{(n)}) \setminus \{\emptyset\}$, since each $e \in \mathcal{E}^{(n)}$ is nonempty.
- 3. $w^{(n)}$ assigns a nonnegative real to each $e \in \mathcal{E}^{(n)}$.

These are exactly the requirements of an n-SuperHypernetwork (cf. Definition of n-SuperHypernetwork), so $H_{\mathrm{sym}}^{(n)}$ qualifies.

Theorem 4.14 (Generalization of Symptom Hypernetwork and Symptom Network). *The Symptom* n-SuperHypernetwork $H_{\text{sym}}^{(n)}$ contains as special cases:

- 1. When n=1, restricting its node-set to singletons $\{\{s_i\}: s_i \in \mathcal{S}\}$ and its hyperedges to subsets of these singletons, one recovers the Symptom Hypernetwork $H_{\text{sym}} = (\mathcal{S}, \mathcal{E}, w)$.
- 2. Further restricting to those hyperedges of size two among singletons yields the classical Symptom Network G = (S, E, W).

Proof. 1. For n=1, $\mathcal{P}^1(\mathcal{S})=\mathcal{P}(\mathcal{S})$. The injection $\iota\colon s_i\mapsto \{s_i\}$ identifies each symptom with a singleton in $V^{(1)}$. Under this identification, the hyperedges of $H^{(1)}_{\mathrm{sym}}$ exactly match those in the Symptom Hypernetwork (since $\mathrm{flat}_1(\{s_i,s_j,\dots\})=\{s_i,s_j,\dots\}$), and weights coincide by definition of $w^{(1)}$.

2. Among those hyperedges, selecting only pairs $\{\{s_i\}, \{s_j\}\}$ corresponds to edges $\{s_i, s_j\}$ in the classical Symptom Network. The associated weight $w^{(1)}(\{\{s_i\}, \{s_j\}\})$ equals $|\operatorname{assoc}(X_i, X_j \mid \mathbf{X}_{\mathcal{S}\setminus \{i, j\}})|$, matching the network weight w_{ij} .

Thus $H_{\mathrm{sym}}^{(n)}$ indeed generalizes both the Symptom Hypernetwork and the underlying Symptom Network. \Box

Theorem 4.15 (Canonical Injection into Higher Orders). For each $n \ge 1$, the map

$$\phi_n: \mathcal{E}^{(n)} \longrightarrow \mathcal{E}^{(n+1)}, \qquad \phi_n(e) = \{e\}$$

is well-defined, injective, and weight-preserving.

Proof. By definition, each $e \in \mathcal{E}^{(n)}$ is a nonempty subset of $\mathcal{P}^n(\mathcal{S})$ with $\left|\operatorname{flat}_n(e)\right| \geq 2$ and $\operatorname{assoc}(X_{\operatorname{flat}_n(e)} \mid \mathbf{X}_{\mathcal{S} \setminus \operatorname{flat}_n(e)}) \neq 0$.

1. Well-defined. $\phi_n(e) = \{e\}$ is a singleton subset of $\mathcal{P}^n(\mathcal{S}) = \mathcal{P}^{(n+1)-1}(\mathcal{S})$, hence $\phi_n(e) \in \mathcal{P}(\mathcal{P}^n(\mathcal{S})) = \mathcal{P}^{n+1}(\mathcal{S})$. Moreover,

$$\left| \operatorname{flat}_{n+1}(\{e\}) \right| = \left| \operatorname{flat}_n(e) \right| \ge 2,$$

and

$$\operatorname{assoc} \left(X_{\operatorname{flat}_{n+1}(\{e\})} \mid \mathbf{X}_{\mathcal{S} \setminus \operatorname{flat}_{n+1}(\{e\})} \right) = \operatorname{assoc} \left(X_{\operatorname{flat}_{n}(e)} \mid \mathbf{X}_{\mathcal{S} \setminus \operatorname{flat}_{n}(e)} \right) \neq 0.$$

Thus $\{e\} \in \mathcal{E}^{(n+1)}$.

- 2. Injectivity. If $\phi_n(e_1) = \phi_n(e_2)$, then $\{e_1\} = \{e_2\}$, so $e_1 = e_2$.
- 3. Weight Preservation. By definition of the weight functions,

$$w^{(n+1)}(\phi_n(e)) = |\operatorname{assoc}(X_{\operatorname{flat}_{n+1}(\{e\})} | \cdots)| = |\operatorname{assoc}(X_{\operatorname{flat}_n(e)} | \cdots)| = w^{(n)}(e).$$

Hence ϕ_n is a canonical injective embedding of $\mathcal{E}^{(n)}$ into $\mathcal{E}^{(n+1)}$, preserving weights.

Theorem 4.16 (Flattening Surjection onto Symptom Hypernetwork). The flattening map

$$\operatorname{flat}_n: \mathcal{E}^{(n)} \longrightarrow \mathcal{E}^{(1)}, \qquad e \mapsto \operatorname{flat}_n(e)$$

is surjective onto the hyperedge-set $\mathcal{E}^{(1)}$ of the Symptom Hypernetwork H_{sym} .

Proof. Let $e' \in \mathcal{E}^{(1)}$ be any hyperedge of the Symptom Hypernetwork. By definition, $e' \subseteq \mathcal{E}$ with $|e'| \geq 2$ and $\operatorname{assoc}(X_{e'} \mid \mathbf{X}_{\mathcal{S} \setminus e'}) \neq 0$. Define $E = \{e'\} \subseteq \mathcal{P}^n(\mathcal{S})$. Then $\operatorname{flat}_n(E) = e'$ and $|\operatorname{flat}_n(E)| = |e'| \geq 2$, while $\operatorname{assoc}(X_{\operatorname{flat}_n(E)} \mid \cdots) = \operatorname{assoc}(X_{e'} \mid \cdots) \neq 0$. Hence $E \in \mathcal{E}^{(n)}$ and $\operatorname{flat}_n(E) = e'$. Since e' was arbitrary, flat_n is surjective onto $\mathcal{E}^{(1)}$.

Theorem 4.17 (Projection to Classical Symptom Network). *Under the identification* $\{s_i, s_j\} \subseteq \mathcal{E}^{(1)}$ *with the edge* $\{s_i, s_j\}$ *in the classical Symptom Network* (\mathcal{S}, E, W) , *the composition* $\operatorname{proj} = \iota_2 \circ \operatorname{flat}_n$ *defined by*

$$proj(e) = \{ \{s_i, s_j\} \in flat_n(e) : i \neq j \},\$$

yields the edge-set E of the classical network and preserves weights.

Proof. By Theorem 4.16, for each $e' \in \mathcal{E}^{(1)}$ there is $e \in \mathcal{E}^{(n)}$ with $\mathrm{flat}_n(e) = e'$. Restricting to pairs $\{s_i, s_j\} \subseteq e'$ recovers exactly those edges with $\mathrm{assoc}(X_i, X_j \mid \mathbf{X}_{\mathcal{S}\setminus\{i,j\}}) \neq 0$. The weight $w_{ij} = \left|\mathrm{assoc}(X_i, X_j \mid \mathbf{X}_{\setminus\{i,j\}})\right|$ coincides with $w^{(n)}(e)$ when e is chosen so that $\mathrm{flat}_n(e) = \{s_i, s_j\}$. Hence proj identifies the classical Symptom Network (\mathcal{S}, E, W) as a projection of the Symptom n-SuperHypernetwork.

Theorem 4.18 (Reduction to Symptom Hypernetwork and Symptom Network). Let $H_{\text{sym}}^{(n)} = (V^{(n)}, \mathcal{E}^{(n)}, w^{(n)})$ be a Symptom n-SuperHypernetwork over base symptom set \mathcal{S} . Then:

1. For n = 1, the restriction

$$V^{(1)} \subseteq \mathcal{P}(\mathcal{S}), \quad \mathcal{E}^{(1)} \subseteq \mathcal{P}(\mathcal{S})$$

recovers the Symptom Hypernetwork $H_{sym} = (S, \mathcal{E}, w)$ under the identification of each singleton $\{s_i\}$ with s_i .

2. For n=0, since $\mathcal{P}^0(\mathcal{S})=\mathcal{S}$, one obtains the classical Symptom Network $G=(\mathcal{S},E,W)$ by taking only those hyperedges of size 2 and interpreting them as edges.

Proof. (1) When $n=1, V^{(1)} \subseteq \mathcal{P}(\mathcal{S})$. Mapping each $s_i \in \mathcal{S}$ to the singleton $\{s_i\} \in V^{(1)}$ identifies the nodes. By definition, $\mathcal{E}^{(1)}$ consists of those subsets of \mathcal{S} with nonzero conditional association, hence coincides with \mathcal{E} . The weights agree by construction of $w^{(1)}$.

(2) When n=0, $\mathcal{P}^0(\mathcal{S})=\mathcal{S}$. Thus $V^{(0)}=\mathcal{S}$ and each hyperedge in $\mathcal{E}^{(0)}\subseteq\mathcal{S}$ of size two becomes an undirected edge in G. The weight function $w^{(0)}$ on pairs coincides with the pairwise association $|\rho_{ij}|$, yielding the classical weighted Symptom Network.

Theorem 4.19 (Skeleton Consistency). For $k = n - 1, n - 2, \dots, 0$, define

$$V^{(k)} = \bigcup_{e \in V^{(k+1)}} e, \quad \mathcal{E}^{(k)} = \{\, f \subseteq V^{(k)} : f \subseteq e \text{ for some } e \in \mathcal{E}^{(k+1)} \}.$$

Then $(V^{(k)}, \mathcal{E}^{(k)}, w^{(k)})$ is a Symptom k-SuperHypernetwork, and in particular yields the Symptom Hypernetwork and Symptom Network at k = 1 and k = 0, respectively.

Proof. By downward induction. For k=n the statement is given. Assuming $(V^{(k+1)},\mathcal{E}^{(k+1)})\subseteq\mathcal{P}^{k+1}(\mathcal{S})$, forming $V^{(k)}$ as unions of those (k+1)-supernodes gives $V^{(k)}\subseteq\mathcal{P}^k(\mathcal{S})$. Each $f\in\mathcal{E}^{(k)}$ lies inside some (k+1)-superedge and hence also inside $\mathcal{P}^k(\mathcal{S})$. The inherited weights $w^{(k)}$ remain nonnegative. Thus by definition it is a Symptom k-SuperHypernetwork. Iterating down to k=1 and k=0 recovers the lower-level models.

Theorem 4.20 (Connectivity Inheritance). If the bipartite incidence graph between $V^{(n)}$ and $\mathcal{E}^{(n)}$ is connected, then for every $1 \leq k \leq n$ the 2-section graph of $(V^{(k)}, \mathcal{E}^{(k)})$ is connected. In particular, the underlying Symptom Network at k = 0 is connected.

Proof. Connectivity of the incidence graph implies that any two k-supernodes are joined by a sequence alternating between supernodes and superedges. Projecting to the 2-section at level k yields a path of adjacent supernodes (sharing at least one (k-1)-supernode). By induction down to k=0, one obtains a path between any two base symptoms in the classical network, proving connectivity inheritance.

Theorem 4.21 (Clique Expansion Representation). Let $G_2 = (\mathcal{S}, E_2, w_2)$ be the 2-section graph of $H_{\mathrm{sym}}^{(n)}$, where

$$E_{2} = \{\{s_{i}, s_{j}\} : \exists e \in \mathcal{E}^{(n)} \text{ with } \{s_{i}, s_{j}\} \subseteq \text{flat}_{n}(e)\},$$

$$w_{2}(\{s_{i}, s_{j}\}) = \max_{\substack{e \in \mathcal{E}^{(n)} \\ \{s_{i}, s_{j}\} \subseteq \text{flat}_{n}(e)}} w^{(n)}(e).$$

Then G_2 is a well-defined weighted Symptom Network that captures every pairwise association implied by higher-order hyperedges.

Proof. Each pair $\{s_i, s_j\}$ appearing in some flattened superedge is included in E_2 . Since $\mathcal{E}^{(n)}$ is finite, the maximum weight is well-defined and nonnegative. This matches the definition of a weighted Symptom Network, hence the clique expansion yields a valid graph. \square

5 CONCLUSION AND FUTURE WORKS

In this paper, We proposed a novel extension classical graph-based models in the medical Specifically, and neuroscientific domains. We analyzed introduced and four higherorder structures: Brain Hypergraphs, Symptom Hypernetworks. Brain Superhypergraphs, Symptom SuperHypernetworks. For each structure, We provided formal mathematical definitions, detailed illustrative examples, and discussions of their theoretical properties.

It is important to note that this study is conceptual and theoretical in nature. While it lays a rigorous foundation, further research is required to explore and validate these frameworks using empirical data. We hope that future studies will pursue such applications through real-world experimentation and clinical datasets.

And as a direction for future work, We aim to explore the integration of advanced uncertaintyhandling frameworks into our proposed models. In particular, We are interested in incorporating: Fuzzy Sets (Zadeh, 1965; Nishad et al., 2023; Zadeh, 2011, 1972), Intuitionistic Fuzzy Sets (Atanassov and Gargov, 1998; Atanassov and Atanassov, 1999; Atanassov, 2012, 2020), Bipolar Fuzzy Sets (Samanta and Pal, 2012; Akram, 2011), m-polar fuzzy Sets (Chen et al., 2014; Kumam et al., 2023; Riaz and Hashmi, 2019), Soft Sets (Maji et al., 2003; Molodtsov, 1999), HyperSoft Sets (Smarandache, 2023a, 2018), Vague Sets (Gau and Buehrer, 1993; Akram et al., 2014; Bustince and Burillo, 1996), Rough Sets (Pawlak, 1982; Pawlak et al., 1988, 1995; Pawlak and Skowron, 2007), HyperRough Sets (Fujita, 2025d,i, 2024a, 2025j), HyperFuzzy Sets (Jun et al., 2017; Song et al., 2017; Ghosh and Samanta, 2012), Picture Fuzzy Sets (Hatamleh et al., 2025; Cuong and Kreinovich, 2013; Das et al., 2022, 2024), Hesitant Fuzzy Sets (Torra and Narukawa, 2009; Torra, 2010; Akram et al., 2019; Farhadinia et al., 2020), Neutrosophic Sets (Smarandache, 1999; Jdid et al., 2023; Smarandache and Salama, 2015), Quadripartitioned Neutrosophic Sets (Fujita and Smarandache, 2025b; Yiarayong, 2024; Khattak et al., 2025; Shi et al., 2023), HyperUncertain Sets (Smarandache, 2017; Fujita, 2025d,f), and Plithogenic Sets (Smarandache and Jdid, 2023; Fujita and Smarandache, 2024b; Fujita, 2025a). These frameworks are expected to further enhance the expressive power and applicability of Hypergraph-based models in handling complex, multi-level uncertainty. In particular, recent studies have demonstrated the effectiveness of Fuzzy Set and Neutrosophic Set theory in medical imaging applications such as MRI analysis (Iqbal et al., 2024; Zhao et al., 2023; Solanki and Kumar, 2023). Based on this trend, We anticipate that future mathematical extensions of Brain Graphs using Fuzzy or Neutrosophic frameworks could yield significant advances in modeling and analyzing brain activity under uncertainty.

6 LIMITATIONS

The theoretical concepts presented in this paper have not yet been subject to practical implementation or empirical validation. Future researchers are invited to explore these ideas in applied or experimental settings.

The results presented are valid only under the specific assumptions and conditions detailed in the manuscript.

Extending these findings to broader mathematical structures may require additional research.

DISCLAIMER (ARTIFICIAL INTELLIGENCE)

Author(s) hereby declare that NO generative AI technologies such as Large Language Models (ChatGPT, COPILOT, etc) and text-to-image generators have been used during writing or editing of manuscripts.

COMPETING INTERESTS

Authors have declared that no competing interests exist.

REFERENCES

- Adebisi, S. A. and Ajuebishi, A. P. (2025). The order involving the neutrosophic hyperstructures, the construction and setting up of a typical neutrosophic group. *HyperSoft Set Methods in Engineering*, 3:26– 31.
- Akram, M. (2011). Bipolar fuzzy graphs. *Information sciences*, 181(24):5548–5564.
- Akram, M., Adeel, A., and Alcantud, J. C. R. (2019). Hesitant fuzzy n-soft sets: A new model with applications in decision-making. *Journal of Intelligent & Fuzzy Systems*, 36(6):6113–6127.
- Akram, M., Gani, A. N., and Saeid, A. B. (2014). Vague hypergraphs. *Journal of Intelligent & Fuzzy Systems*, 26(2):647–653.
- Aksoy, S. G., Joslyn, C., Marrero, C. O., Praggastis, B., and Purvine, E. (2020). Hypernetwork science via high-order hypergraph walks. *EPJ Data Science*, 9(1):16.
- Al-Odhari, A. (2025). A brief comparative study on hyperstructure, super hyperstructure, and n-super superhyperstructure. Neutrosophic Knowledge, 6:38–49.
- Al-Tahan, M., Davvaz, B., Smarandache, F., and Anis, O. (2021). On some neutrohyperstructures. *Symmetry*, 13(4):535.
- Amiri, G., Mousarezaei, R., and Rahnama, S. (2024). Soft hyperstructures and their applications. *New Mathematics and Natural Computation*, pages 1–19.

- An, M. H., Park, S. S., You, S. C., Park, R. W., Park, B., Woo, H. K., Kim, H. K., and Son, S. J. (2019). Depressive symptom network associated with comorbid anxiety in late-life depression. *Frontiers in Psychiatry*, 10.
- An, Z., Tang, K., Xie, Y., Tong, C., Liu, J., Tao, Q., and Feng, Y. (2024). Aberrant resting-state co-activation network dynamics in major depressive disorder. *Translational Psychiatry*, 14.
- Anna Jażdżewska, I. (2022). Use of graph theory to study connectivity and regionalisation of the polish urban network. *Area*, 54(2):290–303.
- Antoni, C. and Braun, J. (2002). Side effects of anti-tnf therapy: current knowledge. *Clinical and experimental rheumatology*, 20(6; SUPP/28):S-152.
- Appert, M. and Laurent, C. (2007). Measuring urban road network vulnerability using graph theory: the case of montpellier's road network. *La mise en carte des risques naturels*, page 89p.
- Atanassov, K. and Gargov, G. (1998). Elements of intuitionistic fuzzy logic. part i. *Fuzzy sets and systems*, 95(1):39–52.
- Atanassov, K. T. (2012). *On intuitionistic fuzzy sets theory*, volume 283. Springer.
- Atanassov, K. T. (2020). Circular intuitionistic fuzzy sets. *Journal of Intelligent & Fuzzy Systems*, 39(5):5981–5986
- Atanassov, K. T. and Atanassov, K. T. (1999). *Intuitionistic fuzzy sets.* Springer.
- Babcock, H. M., Merz, L. R., and Fraser, V. J. (2006). Is influenza an influenza-like illness? clinical presentation of influenza in hospitalized patients. *Infection Control & Hospital Epidemiology*, 27:266 270.
- Balasubramanian, K. and Gupta, S. P. (2019). Quantum molecular dynamics, topological, group theoretical and graph theoretical studies of protein-protein interactions. *Current topics in medicinal chemistry*, 19(6):426–443.
- Bangura, J. B., Xiao, S., Qiu, D., Ouyang, F., and Chen, L. (2020). Barriers to childhood immunization in subsaharan africa: A systematic review. *BMC public* health, 20:1–15.

- Bassett, D. S. and Sporns, O. (2017). Network neuroscience. *Nature neuroscience*, 20(3):353–364.
- Berge, C. (1984). *Hypergraphs: combinatorics of finite sets*, volume 45. Elsevier.
- Bergsneider, B. H., Armstrong, T. S., Conley, Y. P., Cooper, B., Hammer, M., Levine, J. D., Paul, S., Miaskowski, C., and Celiku, O. (2024). Symptom network analysis and unsupervised clustering of oncology patients identifies drivers of symptom burden and patient subgroups with distinct symptom patterns. *Cancer Medicine*, 13(19):e70278.
- Binfalah, M., Alghawi, E., Shosha, E., Alhilly, A. J., and Bakhiet, M. (2018). Sphenopalatine ganglion block for the treatment of acute migraine headache. *Pain Research and Treatment*, 2018.
- Bondy, J. A., Murty, U. S. R., et al. (1976). *Graph theory with applications*, volume 290. Macmillan London.
- Bowler, N., Funk, D., and Slilaty, D. (2020). Describing quasi-graphic matroids. *European Journal of Combinatorics*, 85:103062.
- Bravo, J. C. M., Piedrahita, C. J. B., Bravo, M. A. M., and Pilacuan-Bonete, L. M. (2025). Integrating smed and industry 4.0 to optimize processes with plithogenic n-superhypergraphs. *Neutrosophic Sets and Systems*, 84:328–340.
- Bretto, A. (2013). Hypergraph theory. *An introduction. Mathematical Engineering. Cham: Springer*, 1.
- Brigger, I., Dubernet, C., and Couvreur, P. (2012). Nanoparticles in cancer therapy and diagnosis. *Advanced drug delivery reviews*, 64:24–36.
- Bromfield, S. G., Ngameni, C.-A., Colantonio, L. D.,
 Bowling, C. B., Shimbo, D., Reynolds, K., Safford,
 M. M., Banach, M., Toth, P. P., and Muntner,
 P. (2017). Blood pressure, antihypertensive polypharmacy, frailty, and risk for serious fall injuries among older treated adults with hypertension.
 Hypertension, 70(2):259–266.
- Brown, D. G., Rao, S., Weir, T. L., O'Malia, J., Bazan, M., Brown, R. J., and Ryan, E. P. (2016). Metabolomics and metabolic pathway networks from human colorectal cancers, adjacent mucosa, and stool. *Cancer & metabolism*, 4:1–12.

- Brown, J. M. and Giaccia, A. J. (1998). The unique physiology of solid tumors: opportunities (and problems) for cancer therapy. *Cancer research*, 58(7):1408–1416.
- Bulgakova, V. A., Pshenichnaya, N. Y., Grekova, A. I., Selkova, E. P., Lvov, N. I., Leneva, I. A., Shestakova, I. V., and Maleyev, V. V. (2018). Influenza and influenza-like illnesses in risk groups: evaluation of antiviral therapy with umifenovir in hospitalized patients. *International Journal of Infectious Diseases*.
- Bullmore, E. T. and Bassett, D. S. (2011). Brain graphs: graphical models of the human brain connectome. *Annual review of clinical psychology*, 7(1):113–140.
- Bustince, H. and Burillo, P. (1996). Vague sets are intuitionistic fuzzy sets. Fuzzy sets and systems, 79(3):403–405.
- Cai, D., Song, M., Sun, C., Zhang, B., Hong, S., and Li, H. (2022). Hypergraph structure learning for hypergraph neural networks. In *IJCAI*, pages 1923– 1929.
- Cai, H., Zhou, Z., Yang, D., Wu, G., and Chen, J. (2023). Discovering brain network dysfunction in alzheimer's disease using brain hypergraph neural network. In *International Conference on Medical Image Computing and Computer-Assisted Intervention*.
- Calazans, M. A. A., Ferreira, F. A., Santos, F. A., Madeiro, F., and Lima, J. B. (2024). Machine learning and graph signal processing applied to healthcare: A review. *Bioengineering*, 11(7):671.
- Campbell, J. D. and Burgess, M. (2004). Heterogeneity of pediatric immunization schedules in industrialized countries. *New Generation Vaccines, 3rd edn. Marcel Dekker, New York.*
- Carvalho, C., Santos, R. X., Cardoso, S., Correia, S., Oliveira, P. J., Santos, M. S., and Moreira, P. I. (2009). Doxorubicin: the good, the bad and the ugly effect. *Current medicinal chemistry*, 16(25):3267–3285.
- Castiglioni, A. (2019). A history of medicine. Routledge.
- Cella, D. F., Tulsky, D. S., Gray, G., Sarafian, B., Linn, E., Bonomi, A., Silberman, M., Yellen, S. B., Winicour, P., and Brannon, J. (1993). The functional assessment of cancer therapy scale: development and validation

- of the general measure. *Journal of clinical oncology* : official journal of the American Society of Clinical Oncology, 11 3:570–9.
- Chatterjee, S., Khunti, K., and Davies, M. J. (2017).
 Type 2 diabetes. *The lancet*, 389(10085):2239–2251.
- Chauhan, V. K., Zhou, J., Lu, P., Molaei, S., and Clifton, D. A. (2024). A brief review of hypernetworks in deep learning. Artificial Intelligence Review, 57(9):250.
- Chen, J., Li, S., Ma, S., and Wang, X. (2014). m-polar fuzzy sets: an extension of bipolar fuzzy sets. *The scientific world journal*, 2014(1):416530.
- Chen, J. and Schwaller, P. (2024). Molecular hypergraph neural networks. *The Journal of Chemical Physics*, 160(14).
- Chen, T., Filkov, V., and Skiena, S. S. (1999). Identifying gene regulatory networks from experimental data. In *Proceedings of the third annual international conference on Computational molecular biology*, pages 94–103.
- Chou, T. C. (2006). Theoretical basis, experimental design, and computerized simulation of synergism and antagonism in drug combination studies. *Pharmacological Reviews*, 58:621 681.
- Chou, T. C. (2010). Drug combination studies and their synergy quantification using the chou-talalay method. *Cancer research*, 70 2:440–6.
- Cruz, R., Gutman, I., and Rada, J. (2021). Sombor index of chemical graphs. *Applied Mathematics and Computation*, 399:126018.
- Cuong, B. C. and Kreinovich, V. (2013). Picture fuzzy sets-a new concept for computational intelligence problems. In 2013 third world congress on information and communication technologies (WICT 2013), pages 1–6. IEEE.
- Dabush, L. and Routtenberg, T. (2024). Verifying the smoothness of graph signals: A graph signal processing approach. IEEE Transactions on Signal Processing.
- Das, A. K., Das, R., Das, S., Debnath, B. K., Granados, C., Shil, B., and Das, R. (2025). A comprehensive study of neutrosophic superhyper bci-semigroups and their algebraic significance. *Transactions on Fuzzy Sets and Systems*, 8(2):80.

- Das, S., Ghorai, G., and Pal, M. (2022). Picture fuzzy tolerance graphs with application. *Complex & Intelligent Systems*, 8(1):541–554.
- Das, S., Poulik, S., and Ghorai, G. (2024). Picture fuzzy φ-tolerance competition graphs with its application. Journal of Ambient Intelligence and Humanized Computing, 15(1):547–559.
- DeFronzo, R. A., Ferrannini, E., Groop, L., Henry, R. R., Herman, W. H., Holst, J. J., Hu, F. B., Kahn, C. R., Raz, I., Shulman, G. I., et al. (2015). Type 2 diabetes mellitus. *Nature reviews Disease primers*, 1(1):1–22.
- Deo, N. (2016). Graph theory with applications to engineering and computer science. Courier Dover Publications.
- DeVita Jr, V. T. and Chu, E. (2008). A history of cancer chemotherapy. *Cancer research*, 68(21):8643–8653.
- Diestel, R. Graduate texts in mathematics: Graph theory.
- Diestel, R. (2005). Graph theory 3rd ed. *Graduate texts in mathematics*, 173(33):12.
- Ding, Y., Tang, J., and Guo, F. (2019). Identification of drug-side effect association via multiple information integration with centered kernel alignment. *Neurocomputing*, 325:211–224.
- Falster, M. O., Buckley, N. A., Brieger, D., and Pearson, S.-A. (2020). Antihypertensive polytherapy in australia: prevalence of inappropriate combinations, 2013–2018. *Journal of Hypertension*, 38(8):1586– 1592.
- Farhadinia, B., Aickelin, U., and Khorshidi, H. A. (2020). Uncertainty measures for probabilistic hesitant fuzzy sets in multiple criteria decision making. *International Journal of Intelligent Systems*, 35(11):1646–1679.
- Feng, Y., You, H., Zhang, Z., Ji, R., and Gao, Y. (2019). Hypergraph neural networks. In *Proceedings of the AAAI conference on artificial intelligence*, volume 33, pages 3558–3565.
- Foulds, L. R. (1995). *Graph theory applications*. Springer Science & Business Media.
- Fried, M. W. (2002). Side effects of therapy of hepatitis c and their management. *Hepatology*, 36(S1):S237—S244.

- Fujita, T. (2024a). Hyperrough cubic set and superhyperrough cubic set. *Prospects for Applied Mathematics and Data Analysis*, 4(1):28–35.
- Fujita, T. (2024b). Review of some superhypergraph classes: Directed, bidirected, soft, and rough. Advancing Uncertain Combinatorics through Graphization, Hyperization, and Uncertainization: Fuzzy, Neutrosophic, Soft, Rough, and Beyond (Second Volume).
- Fujita, T. (2025a). Advancing Uncertain Combinatorics through Graphization, Hyperization, and Uncertainization: Fuzzy, Neutrosophic, Soft, Rough, and Beyond. Biblio Publishing.
- Fujita, T. (2025b). Antihyperstructure, neutrohyperstructure, and superhyperstructure. Advancing Uncertain Combinatorics through Graphization, Hyperization, and Uncertainization: Fuzzy, Neutrosophic, Soft, Rough, and Beyond, page 311.
- Fujita, T. (2025c). Exploration of graph classes and concepts for superhypergraphs and n-th power mathematical structures. Advancing Uncertain Combinatorics through Graphization, Hyperization, and Uncertainization: Fuzzy, Neutrosophic, Soft, Rough, and Beyond, 3(4):512.
- Fujita, T. (2025d). Forest hyperplithogenic set and forest hyperrough set. Advancing Uncertain Combinatorics through Graphization, Hyperization, and Uncertainization: Fuzzy, Neutrosophic, Soft, Rough, and Beyond.
- Fujita, T. (2025e). Hypergraph and superhypergraph approaches in electronics: A hierarchical framework for modeling power-grid hypernetworks and superhypernetworks. *Journal of Energy Research and Reviews*, 17(6):102–136.
- Fujita, T. (2025f). Hyperplithogenic cubic set and superhyperplithogenic cubic set. Advancing Uncertain Combinatorics through Graphization, Hyperization, and Uncertainization: Fuzzy, Neutrosophic, Soft, Rough, and Beyond, page 79.
- Fujita, T. (2025g). An introduction and reexamination of molecular hypergraph and molecular n-superhypergraph. Asian Journal of Physical and Chemical Sciences, 13(3):1–38.

- Fujita, T. (2025h). Modeling hierarchical systems in graph signal processing, electric circuits, and bond graphs via hypergraphs and superhypergraphs. *Journal of Engineering Research and Reports*, 27(5):542.
- Fujita, T. (2025i). Neighborhood hyperrough set and neighborhood superhyperrough set. *Pure Mathematics for Theoretical Computer Science*, 5(1):34–47.
- Fujita, T. (2025j). Short introduction to rough, hyperrough, superhyperrough, treerough. Advancing Uncertain Combinatorics through Graphization, Hyperization, and Uncertainization: Fuzzy, Neutrosophic, Soft, Rough, and Beyond: Fifth volume: Various SuperHyperConcepts (Collected Papers), page 394.
- Fujita, T. (2025k). A theoretical investigation of quantum n-superhypergraph states. *Neutrosophic Optimization and Intelligent Systems*, 6:15–25.
- Fujita, T. (2025l). Unifying grain boundary networks and crystal graphs: A hypergraph and superhypergraph perspective in material sciences. *Asian Journal of Advanced Research and Reports*, 19(5):344–379.
- Fujita, T. and Smarandache, F. A reconsideration of advanced concepts in neutrosophic graphs: Smart, zero divisor, layered, weak, semi, and chemical graphs. Advancing Uncertain Combinatorics through Graphization, Hyperization, and Uncertainization: Fuzzy, Neutrosophic, Soft, Rough, and Beyond, page 308
- Fujita, T. and Smarandache, F. (2024a). A concise study of some superhypergraph classes. *Neutrosophic Sets and Systems*, 77:548–593.
- Fujita, T. and Smarandache, F. (2024b). A review of the hierarchy of plithogenic, neutrosophic, and fuzzy graphs: Survey and applications. In Advancing Uncertain Combinatorics through Graphization, Hyperization, and Uncertainization: Fuzzy, Neutrosophic, Soft, Rough, and Beyond (Second Volume). Biblio Publishing.
- Fujita, T. and Smarandache, F. (2025a). Fundamental computational problems and algorithms for superhypergraphs. *HyperSoft Set Methods in Engineering*, 3:32–61.

- Fujita, T. and Smarandache, F. (2025b). Some types of hyperneutrosophic set (3): Dynamic, quadripartitioned, pentapartitioned, heptapartitioned, m-polar. Advancing Uncertain Combinatorics through Graphization, Hyperization, and Uncertainization: Fuzzy, Neutrosophic, Soft, Rough, and Beyond, page 178.
- Fujita, T. and Smarandache, F. (2025c). Superhypergraph neural networks and plithogenic graph neural networks: Theoretical foundations. Advancing Uncertain Combinatorics through Graphization, Hyperization, and Uncertainization: Fuzzy, Neutrosophic, Soft, Rough, and Beyond.
- Gau, W.-L. and Buehrer, D. J. (1993). Vague sets. *IEEE transactions on systems, man, and cybernetics*, 23(2):610–614.
- Ghosh, J. and Samanta, T. K. (2012). Hyperfuzzy sets and hyperfuzzy group. *Int. J. Adv. Sci. Technol*, 41:27–37.
- Gilmore, B. and Michael, M. (2011a). Treatment of acute migraine headache. *American family physician*, 83 3:271–280.
- Gilmore, B. and Michael, M. (2011b). Treatment of acute migraine headache. American family physician, 83(3):271–280.
- Goodwin, J. S., Hunt, W. C., Humble, C. G., Key, C. R., and Samet, J. M. (1988). Cancer treatment protocols: who gets chosen? *Archives of internal medicine*, 148(10):2258–2260.
- Gotay, C. C., Korn, E. L., McCabe, M. S., Moore, T. D., and Cheson, B. D. (1992). Quality-of-life assessment in cancer treatment protocols: research issues in protocol development. *JNCI: Journal of the National Cancer Institute*, 84(8):575–579.
- Gottlob, G. and Pichler, R. (2004). Hypergraphs in model checking: Acyclicity and hypertree-width versus clique-width. *SIAM Journal on Computing*, 33(2):351–378.
- Gross, J. L., Yellen, J., and Anderson, M. (2018). *Graph theory and its applications*. Chapman and Hall/CRC.
- Gupta, R. and Guptha, S. (2010). Strategies for initial management of hypertension. *indian Journal of medical research*, 132(5):531–542.

- Ha, D., Dai, A., and Le, Q. V. (2016). Hypernetworks. arXiv preprint arXiv:1609.09106.
- Hamidi, M., Smarandache, F., and Taghinezhad, M. (2023). *Decision Making Based on Valued Fuzzy Superhypergraphs*. Infinite Study.
- Hansen, J. M., Lipton, R. B., Dodick, D. W., Silberstein, S. D., Saper, J. R., Aurora, S. K., Goadsby, P. J., and Charles, A. (2012). Migraine headache is present in the aura phase: a prospective study. *Neurology*, 79(20):2044–2049.
- Harvey, D. J. and Wood, D. R. (2017). Parameters tied to treewidth. *Journal of Graph Theory*, 84(4):364–385.
- Hatamleh, R., Al-Husban, A., Zubair, S. A. M., Elamin, M., Saeed, M. M., Abdolmaleki, E., Fujita, T., Nordo, G., and Khattak, A. M. (2025). Ai-assisted wearable devices for promoting human health and strength using complex interval-valued picture fuzzy soft relations. European Journal of Pure and Applied Mathematics, 18(1):5523–5523.
- Hausdorff, F. (2021). *Set theory*, volume 119. American Mathematical Soc.
- Hempler, I., Woitha, K., Thielhorn, U., and Farin, E. (2018). Post-stroke care after medical rehabilitation in germany: a systematic literature review of the current provision of stroke patients. *BMC health services research*, 18:1–9.
- Henderson, J. M. (2001). A sensorimotor account of vision and visual consciousness. *The Behavioral and brain sciences*, 24 5:939–73; discussion 973–1031.
- Huang, Y., Chen, G., Wen, X., and Shen, D. (2024). Multi-modal brain graph learning of shared-specific features for schizophrenia diagnosis. In 2024 IEEE International Conference on Bioinformatics and Biomedicine (BIBM), pages 1522–1525. IEEE.
- Iqbal, S., Qureshi, A. N., Aurangzeb, K., Alhussein, M. A., Wang, S., Anwar, M. S., and Khan, F. (2024). Hybrid parallel fuzzy cnn paradigm: Unmasking intricacies for accurate brain mri insights. *IEEE Transactions on Fuzzy Systems*, 32:5533–5544.
- Jdid, M., Smarandache, F., and Broumi, S. (2023). Inspection assignment form for product quality control using neutrosophic logic. Infinite Study.
- Jech, T. (2003). Set theory: The third millennium edition, revised and expanded. Springer.

- Johansson, M. A., Quandelacy, T. M., Kada, S., Prasad, P. V., Steele, M., Brooks, J. T., Slayton, R. B., Biggerstaff, M., and Butler, J. C. (2021). Sarscov-2 transmission from people without covid-19 symptoms. *JAMA Network Open*, 4.
- Jun, Y. B., Hur, K., and Lee, K. J. (2017). Hyperfuzzy subalgebras of bck/bci-algebras. Annals of Fuzzy Mathematics and Informatics.
- Kaiser, R. H., Kang, M. S., Lew, Y., Feen, J. V. D., Aguirre, B., Clegg, R., Goer, F., Esposito, E. C., Auerbach, R. P., Hutchison, R. M., and Pizzagalli, D. A. (2019). Abnormal frontoinsular-default network dynamics in adolescent depression and rumination: a preliminary resting-state co-activation pattern analysis. *Neuropsychopharmacology*, pages 1–9.
- Karimi, N., Tavakoli, M., Charati, J. Y., and Shamsizade, M. (2017). Single-dose intravenous sodium valproate (depakine) versus dexamethasone for the treatment of acute migraine headache: a double-blind randomized clinical trial. *Clinical and Experimental Emergency Medicine*, 4:138 145.
- Karlebach, G. and Shamir, R. (2008). Modelling and analysis of gene regulatory networks. *Nature reviews Molecular cell biology*, 9(10):770–780.
- Kelly, H. A. and Birch, C. J. (2004). The causes and diagnosis of influenza-like illness. *Australian family physician*, 33 5:305–9.
- Kerr, J. F., Winterford, C. M., and Harmon, B. V. (1994). Apoptosis. its significance in cancer and cancer therapy. *Cancer*, 73(8):2013–2026.
- Khattak, A. M., Arslan, M., Shihadeh, A., Salameh,
 W. M. M., Al-Husban, A. A.-H., Seethalakshmi,
 R., Nordo, G., Fujita, T., and Saeed, M. M.
 (2025). A breakthrough approach to quadri-partitioned neutrosophic softtopological spaces.
 European Journal of Pure and Applied Mathematics,
 18(2):5845–5845.
- Kocbek, S. and Kim, J.-D. (2017). Exploring biomedical ontology mappings with graph theory methods. *PeerJ*, 5:e2990.
- Koh, G. C., Porras, P., Aranda, B., Hermjakob, H., and Orchard, S. E. (2012). Analyzing protein–protein interaction networks. *Journal of proteome research*, 11(4):2014–2031.

- Kumam, W., Naeem, K., Riaz, M., Khan, M. J., and Kumam, P. (2023). Comparison measures for pythagorean \$ m \$-polar fuzzy sets and their applications to robotics and movie recommender system. AIMS Mathematics.
- Lee, M. H., Smyser, C. D., and Shimony, J. S. (2013). Resting-state fmri: a review of methods and clinical applications. *American Journal of neuroradiology*, 34(10):1866–1872.
- Levy, A. (2012). Basic set theory. Courier Corporation.
- Li, M., Shi, X., Qiao, C., Zhang, T., and Jin, H. (2024). Hyperbolic hypergraph neural networks for multi-relational knowledge hypergraph representation. arXiv preprint arXiv:2412.12158.
- Li, M. M., Huang, K., and Zitnik, M. (2022). Graph representation learning in biomedicine and healthcare. *Nature Biomedical Engineering*, 6(12):1353–1369.
- Li, Z., Han, P., You, Z., Li, X., Zhang, Y., Yu, H., Nie, R., and Chen, X. (2017). In silico prediction of drugtarget interaction networks based on drug chemical structure and protein sequences. *Scientific Reports*, 7.
- Linden, D. E. J. (2007). The working memory networks of the human brain. *The Neuroscientist*, 13:257 267.
- Linial, N. (1992). Locality in distributed graph algorithms. SIAM Journal on computing, 21(1):193– 201.
- Loehrer, P. J. and EINHORN, L. H. (1984). Cisplatin. *Annals of internal medicine*, 100(5):704–713.
- Longley, D. B., Harkin, D. P., and Johnston, P. G. (2003). 5-fluorouracil: mechanisms of action and clinical strategies. *Nature reviews cancer*, 3(5):330–338.
- Luo, X., Wu, J., Yang, J., Xue, S., Beheshti, A., Sheng, Q. Z., McAlpine, D., Sowman, P., Giral, A., and Yu, P. S. (2024). Graph neural networks for brain graph learning: A survey. arXiv preprint arXiv:2406.02594.
- Madhamshettiwar, P. B., Maetschke, S. R., Davis,
 M. J., Reverter, A., and Ragan, M. A. (2012).
 Gene regulatory network inference: evaluation and application to ovarian cancer allows the prioritization of drug targets. *Genome medicine*, 4:1–16.

- Maji, P. K., Biswas, R., and Roy, A. R. (2003). Soft set theory. *Computers & mathematics with applications*, 45(4-5):555–562.
- Mathew, J. L. (2012). Inequity in childhood immunization in india: a systematic review. *Indian pediatrics*, 49:203–223.
- McAllister, T. W., Saykin, A. J., Flashman, L. A., Sparling, M. B., Johnson, S. C., Guerin, S. J., Mamourian, A. C., Weaver, J. B., and Yanofsky, N. N. (1999). Brain activation during working memory 1 month after mild traumatic brain injury. *Neurology*, 53:1300 1300.
- Mhembere, D., Roncal, W. G., Sussman, D., Priebe, C. E., Jung, R., Ryman, S., Vogelstein, R. J., Vogelstein, J. T., and Burns, R. (2013). Computing scalable multivariate glocal invariants of large (brain) graphs. In 2013 IEEE Global Conference on Signal and Information Processing, pages 297–300. IEEE.
- Milone, D. H., Stegmayer, G., López, M., Kamenetzky, L., and Carrari, F. (2014). Improving clustering with metabolic pathway data. *BMC bioinformatics*, 15:1– 10.
- Molodtsov, D. (1999). Soft set theory-first results. *Computers & mathematics with applications*, 37(4-5):19–31.
- Nair, C. K., Parida, D. K., and Nomura, T. (2001). Radioprotectors in radiotherapy. *Journal of radiation research*, 42(1):21–37.
- Nguyen, H. C., Nguyen, M. H., Do, B. N., Tran, C. Q., Nguyen, T. T. P., Pham, K. M., Pham, L. V., Tran, K. V., Duong, T. T., Tran, T. V., Duong, T. H., Nguyen, T. T., Nguyen, Q. H., Hoang, T. M., Nguyen, K. T., Pham, T. T. M., Yang, S.-H., Chao, J. C.-J., and Duong, T. V. (2020). People with suspected covid-19 symptoms were more likely depressed and had lower health-related quality of life: The potential benefit of health literacy. *Journal of Clinical Medicine*, 9.
- Nishad, T., Al-Hawary, T. A., and Harif, B. M. (2023). General fuzzy graphs. *Ratio Mathematica*, 47.
- Pai, S. and Bader, G. D. (2018). Patient similarity networks for precision medicine. *Journal of molecular biology*, 430(18):2924–2938.

- Pai, S., Hui, S., Isserlin, R., Shah, M. A., Kaka, H., and Bader, G. D. (2019). netdx: interpretable patient classification using integrated patient similarity networks. *Molecular systems biology*, 15(3):e8497.
- Pain, S., Sarma, M., and Samanta, D. (2025). Graph signal processing and graph learning approaches to schizophrenia pattern identification in brain electroencephalogram. *Biomedical Signal Processing and Control*, 100:106954.
- Park, C. W. and Wolverton, C. (2020). Developing an improved crystal graph convolutional neural network framework for accelerated materials discovery. *Physical Review Materials*, 4(6):063801.
- Pauwels, E., Stoven, V., and Yamanishi, Y. (2011). Predicting drug side-effect profiles: a chemical fragment-based approach. *BMC Bioinformatics*, 12:169 169.
- Pawlak, Z. (1982). Rough sets. *International journal of computer & information sciences*, 11:341–356.
- Pawlak, Z., Grzymala-Busse, J., Slowinski, R., and Ziarko, W. (1995). Rough sets. *Communications of the ACM*, 38(11):88–95.
- Pawlak, Z. and Skowron, A. (2007). Rudiments of rough sets. *Information sciences*, 177(1):3–27.
- Pawlak, Z., Wong, S. K. M., Ziarko, W., et al. (1988). Rough sets: probabilistic versus deterministic approach. *International Journal of Man-Machine Studies*, 29(1):81–95.
- Peer, D., Karp, J. M., Hong, S., Farokhzad, O. C., Margalit, R., and Langer, R. (2020a). Nanocarriers as an emerging platform for cancer therapy. *Nanoenabled medical applications*, pages 61–91.
- Peer, D., Karp, J. M., Hong, S., Farokhzad, O. C., Margalit, R., and Langer, R. S. (2020b). Nanocarriers as an emerging platform for cancer therapy. *Nano-Enabled Medical Applications*.
- Peghin, M., Palese, A., Venturini, M., Martino, M. D., Gerussi, V., Graziano, E., Bontempo, G., Marrella, F., Tommasini, A., Fabris, M., Curcio, F., Isola, M., and Tascini, C. (2021). Post-covid-19 symptoms 6 months after acute infection among hospitalized and non-hospitalized patients. *Clinical Microbiology and Infection*, 27:1507 – 1513.

- Pisarchik, A. N., Serrano, N. P., and Jaimes-reategui, R. (2024). Brain connectivity hypergraphs. 2024 8th Scientific School Dynamics of Complex Networks and their Applications (DCNA).
- Rajsic, S., Gothe, H., Borba, H., Sroczynski, G., Vujicic, J., Toell, T., and Siebert, U. (2019). Economic burden of stroke: a systematic review on post-stroke care. *The European Journal of Health Economics*, 20:107– 134.
- Raman, K. (2010). Construction and analysis of protein–protein interaction networks. *Automated experimentation*, 2:1–11.
- Riaz, M. and Hashmi, M. R. (2019). Soft rough pythagorean m-polar fuzzy sets and pythagorean m-polar fuzzy soft rough sets with application to decision-making. *Computational and Applied Mathematics*, 39.
- Robertson, N. and Seymour, P. D. (1986). Graph minors. ii. algorithmic aspects of tree-width. *Journal* of algorithms, 7(3):309–322.
- Roobini, M., Jebaraj, M. S., Sasirudh, P., Babu, K., and Muneera, M. N. (2024). Brain graph super-resolution for enhanced neurological disorder diagnosis. In 2024 International Conference on Innovative Computing, Intelligent Communication and Smart Electrical Systems (ICSES), pages 1–12. IEEE.
- Russo, M. W. and Fried, M. W. (2003). Side effects of therapy for chronic hepatitis c. *Gastroenterology*, 124(6):1711–1719.
- Safari-Alighiarloo, N., Taghizadeh, M., Rezaei-Tavirani, M., Goliaei, B., and Peyvandi, A. A. (2014). Proteinprotein interaction networks (ppi) and complex diseases. Gastroenterology and Hepatology from bed to bench, 7(1):17.
- Samanta, S. and Pal, M. (2012). Bipolar fuzzy hypergraphs. *International Journal of Fuzzy Logic Systems*, 2(1):17–28.
- Schumacher, L., Burger, J., Echterhoff, J., and Kriston, L. (2024). Methodological and statistical practices of using symptom networks to evaluate mental health interventions: a review and reflections. *Multivariate Behavioral Research*, 59(4):663–676.

- Semenza, G. L. (2003). Targeting hif-1 for cancer therapy. *Nature Reviews Cancer*, 3:721–732.
- Senger, K., Heider, J., Kleinstäuber, M., Sehlbrede, M., Witthöft, M., and Schröder, A. (2022). Network analysis of persistent somatic symptoms in two clinical patient samples. *Psychosomatic Medicine*, 84(1):74–85.
- Seymour, P. D. (1981). Recognizing graphic matroids. *Combinatorica*, 1:75–78.
- Shi, X., Kosari, S., Rashmanlou, H., Broumi, S., and Satham Hussain, S. (2023). Properties of intervalvalued quadripartitioned neutrosophic graphs with real-life application. *Journal of Intelligent & Fuzzy Systems*, 44(5):7683–7697.
- Sigerist, H. E. (1987). A history of medicine, volume 2. Oxford University Press.
- Singla, A. K., Garg, A., and Aggarwal, D. (2002). Paclitaxel and its formulations. *International journal of pharmaceutics*, 235(1-2):179–192.
- Smarandache, F. (1999). A unifying field in logics: Neutrosophic logic. In *Philosophy*, pages 1–141. American Research Press.
- Smarandache, F. (2017). Hyperuncertain, superuncertain, and superhyperuncertain sets/logics/probabilities/statistics. Infinite Study.
- Smarandache, F. (2018). Extension of soft set to hypersoft set, and then to plithogenic hypersoft set. *Neutrosophic sets and systems*, 22(1):168–170.
- Smarandache, F. (2019). n-superhypergraph and plithogenic n-superhypergraph. *Nidus Idearum*, 7:107–113.
- Smarandache, F. (2020). Extension of HyperGraph to n-SuperHyperGraph and to Plithogenic n-SuperHyperGraph, and Extension of HyperAlgebra to n-ary (Classical-/Neutro-/Anti-) HyperAlgebra. Infinite Study.
- Smarandache, F. (2022a). Introduction to superhyperalgebra and neutrosophic superhyperalgebra. *Journal of Algebraic Hyperstructures and Logical Algebras*.
- Smarandache, F. (2022b). Introduction to the n-SuperHyperGraph-the most general form of graph today. Infinite Study.

- Smarandache, F. (2023a). Foundation of the superhypersoft set and the fuzzy extension superhypersoft set: A new vision. *Neutrosophic Systems with Applications*, 11:48–51.
- Smarandache, F. (2023b). SuperHyperFunction, SuperHyperStructure, Neutrosophic SuperHyperFunction and Neutrosophic SuperHyperStructure: Current understanding and future directions. Infinite Study.
- Smarandache, F. (2024a). The cardinal of the m-powerset of a set of n elements used in the superhyperstructures and neutrosophic superhyperstructures. *Systems Assessment and Engineering Management*, 2:19–22.
- Smarandache, F. (2024b). Foundation of superhyperstructure & neutrosophic superhyperstructure. *Neutrosophic Sets and Systems*, 63(1):21.
- Smarandache, F. (2024c). Superhyperstructure & neutrosophic superhyperstructure. Accessed: 2024-12-01.
- Smarandache, F. and Jdid, M. (2023). An overview of neutrosophic and plithogenic theories and applications.
- Smarandache, F. and Salama, A. (2015). Neutrosophic crisp set theory.
- Smith, S. M., Vidaurre, D., Beckmann, C. F., Glasser, M. F., Jenkinson, M., Miller, K. L., Nichols, T. E., Robinson, E. C., Salimi-Khorshidi, G., Woolrich, M. W., et al. (2013). Functional connectomics from resting-state fmri. *Trends in cognitive sciences*, 17(12):666–682.
- Smitha, K. A., Akhil Raja, K., Arun, K., Rajesh, P., Thomas, B., Kapilamoorthy, T., and Kesavadas, C. (2017). Resting state fmri: A review on methods in resting state connectivity analysis and resting state networks. *The neuroradiology journal*, 30(4):305–317.
- Solanki, R. and Kumar, D. (2023). Probabilistic intuitionistic fuzzy c-means algorithm with spatial constraint for human brain mri segmentation. *Multimedia Tools and Applications*, pages 1–30.

- Song, S.-Z., Kim, S. J., and Jun, Y. B. (2017). Hyperfuzzy ideals in bck/bci-algebras. *Mathematics*, 5(4):81.
- Speck-Planche, A. and Cordeiro, M. (2013). Evolution of graph theory-based qsar methods and their applications to the search for new antibacterial agents. *Current Topics in Medicinal Chemistry*, 13(24):3101–3117.
- Sporns, O. (2018). Graph theory methods: applications in brain networks. *Dialogues in clinical neuroscience*, 20(2):111–121.
- Squire, L., Berg, D., Bloom, F. E., Du Lac, S., Ghosh, A., and Spitzer, N. C. (2012). *Fundamental neuroscience*. Academic press.
- Stephens, F. O., Aigner, K. R., Allen-Mersh, T. G., et al. (2009). *Basics of oncology*. Springer.
- Stewart, W. F., Lipton, R. B., Celentano, D. D., and Reed, M. L. (1992). Prevalence of migraine headache in the united states: relation to age, income, race, and other sociodemographic factors. *Jama*, 267(1):64–69.
- Swathika, O. G., Angalaeswari, S., Krishnan, V. A., Jamuna, K., and Daya, J. F. (2017). Fuzzy decision and graph algorithms aided adaptive protection of microgrid. *Energy Procedia*, 117:1078–1084.
- Tanoli, Z., Alam, Z., Ianevski, A., Wennerberg, K., Vähä-Koskela, M., and Aittokallio, T. (2018). Interactive visual analysis of drug-target interaction networks using drug target profiler, with applications to precision medicine and drug repurposing. *Briefings* in bioinformatics.
- Tedla, Y. G. and Bautista, L. E. (2016). Drug side effect symptoms and adherence to antihypertensive medication. American journal of hypertension, 29 6:772–9.
- Thiede, E. H., Zhou, W., and Kondor, R. (2022). Graph neural networks for biochemistry that incorporate substructure. *Biophysical Journal*.
- Till, S. J., Francis, J. N., Nouri-Aria, K., and Durham, S. R. (2004). Mechanisms of immunotherapy. *Journal of Allergy and Clinical Immunology*, 113(6):1025–1034.
- Torra, V. (2010). Hesitant fuzzy sets. *International* journal of intelligent systems, 25(6):529–539.

- Torra, V. and Narukawa, Y. (2009). On hesitant fuzzy sets and decision. In 2009 IEEE international conference on fuzzy systems, pages 1378–1382. IEEE.
- Trinajstic, N. (2018). *Chemical graph theory*. CRC press.
- Valencia, E. M. C., Vásquez, J. P. C., and Lois, F. Á. B. (2025). Multineutrosophic analysis of the relationship between survival and business growth in the manufacturing sector of azuay province, 2020–2023, using plithogenic n-superhypergraphs. *Neutrosophic Sets and Systems*, 84:341–355.
- van Borkulo, C., Boschloo, L., Borsboom, D., Penninx, B. W., Waldorp, L. J., and Schoevers, R. A. (2015). Association of symptom network structure with the course of depression. *JAMA psychiatry*, 72(12):1219–1226.
- Velickovic, P., Ying, R., Padovano, M., Hadsell, R., and Blundell, C. (2019). Neural execution of graph algorithms. ArXiv, abs/1910.10593.
- Venhorst, J., Núnez, S., and Kruse, C. G. (2010). Design of a high fragment efficiency library by molecular graph theory. ACS Medicinal Chemistry Letters, 1(9):499–503.
- Verma, N., Rastogi, S., Chia, Y.-C., Siddique, S., Turana, Y., Cheng, H.-m., Sogunuru, G. P., Tay, J. C., Teo, B. W., Wang, T.-D., et al. (2021). Nonpharmacological management of hypertension. *The Journal of Clinical Hypertension*, 23(7):1275–1283.
- Vijan, S. (2010). Type 2 diabetes. *Annals of internal medicine*, 152(5):ITC3–1.
- Vougioukli, S. (2020a). Helix hyperoperation in teaching research. *Science & Philosophy*, 8(2):157–163.
- Vougioukli, S. (2020b). Hyperoperations defined on sets of s -helix matrices.
- Vougioukli, S. (2023). Helix-hyperoperations on lie-santilli admissibility. *Algebras Groups and Geometries*.
- Wang, Z.-H., Zheng, X., Rao, G.-W., and Zheng, Q. (2024). Targeted small molecule therapy and inhibitors for lymphoma. *Future Medicinal Chemistry*, 16(14):1465–1484.

- Whitehead, S. and Baalbergen, E. (2019). Poststroke rehabilitation. *South African Medical Journal*, 109(2):81–83.
- Wolpert, D. M., Ghahramani, Z., and Jordan, M. I. (1995). An internal model for sensorimotor integration. *Science*, 269:1880–2.
- Wu, K., Song, X., and Chai, L. (2022). Graph metrics based brain hypergraph learning in schizophrenia patients. *2022 China Automation Congress (CAC)*, pages 3251–3256.
- Xie, T. and Grossman, J. C. (2018). Crystal graph convolutional neural networks for an accurate and interpretable prediction of material properties. *Physical review letters*, 120(14):145301.
- Xu, Z., Li, Q., Zhang, C., Wang, P., Xu, X., Ran, L., Zhang, L., Tian, G., and Zhang, G. (2022). Amorphous ferric oxide-coating selenium core–shell nanoparticles: a self-preservation pt (iv) platform for multi-modal cancer therapies through hydrogen peroxide depletion-mediated antiangiogenesis, apoptosis and ferroptosis. *Nanoscale*, 14(32):11600–11611.
- Yamanishi, Y., Araki, M., Gutteridge, A., Honda, W., and Kanehisa, M. (2008). Prediction of drug-target interaction networks from the integration of chemical and genomic spaces. *Bioinformatics*, 24:i232 i240.
- Yiarayong, P. (2024). Some weighted aggregation operators of quadripartitioned single-valued trapezoidal neutrosophic sets and their multi-criteria group decision-making method for developing green supplier selection criteria. OPSEARCH, pages 1–55.
- Yu, Q., Du, Y., Chen, J., Sui, J., Adalē, T., Pearlson, G. D., and Calhoun, V. D. (2018). Application of graph theory to assess static and dynamic brain connectivity: Approaches for building brain graphs. *Proceedings of the IEEE*, 106(5):886–906.
- Zadeh, L. A. (1965). Fuzzy sets. *Information and control*, 8(3):338–353.
- Zadeh, L. A. (1972). A fuzzy-set-theoretic interpretation of linguistic hedges.

- Zadeh, L. A. (2011). A note on z-numbers. *Information sciences*, 181(14):2923–2932.
- Zhang, H. (2017). Structural analysis of bus networks using indicators of graph theory and complex network theory. *The Open Civil Engineering Journal*, 11(1).
- Zhao, Y., Huang, Z., Che, H., Xie, F., Liu, M., Wang, M., and Sun, D. (2023). Segmentation of brain tissues from mri images using multitask fuzzy clustering algorithm. *Journal of Healthcare Engineering*, 2023.
- Zhou, F., Shefer, A., Wenger, J., Messonnier, M., Wang, L. Y., Lopez, A., Moore, M., Murphy, T. V., Cortese, M., and Rodewald, L. (2014). Economic evaluation of the routine childhood immunization program in the united states, 2009. *Pediatrics*, 133(4):577–585.
- Zhu, Z., Sun, Y., Kuang, Y., Yuan, X., Gu, H., Zhu, J., and Xing, W. (2023). Contemporaneous symptom networks of multidimensional symptom experiences in cancer survivors: a network analysis. *Cancer Medicine*, 12(1):663–673.

Disclaimer/Publisher's Note: The statements, opinions and data contained in all publications are solely those of the individual author(s) and contributor(s) and not of the publisher and/or the editor(s). This publisher and/or the editor(s) disclaim responsibility for any injury to people or property resulting from any ideas, methods, instructions or products referred to in the content.

© Copyright (2025): Author(s). The licensee is the journal publisher. This is an Open Access article distributed under the terms of the Creative Commons Attribution License (http://creativecommons.org/licenses/by/4.0), which permits unrestricted use, distribution, and reproduction in any medium, provided the original work is properly cited.

Peer-review history:
The peer review history for this paper can be accessed here:
https://pr.sdiarticle5.com/review-history/136474